AD-A036 127 NORTHWESTERN UNIV EVANSTON ILL DEPT OF MATERIALS SCI--ETC F/G 20/2
EVALUATION OF PROCEDURES IN AUTOMATED RESIDUAL STRESS MEASUREME--ETC(U)
FEB 77 M R JAMES, J B COHEN N00014-75-C-0580
UNCLASSIFIED TR-14 NL

1 OF 1
AD A036127

END

DATE FILMED
3-77

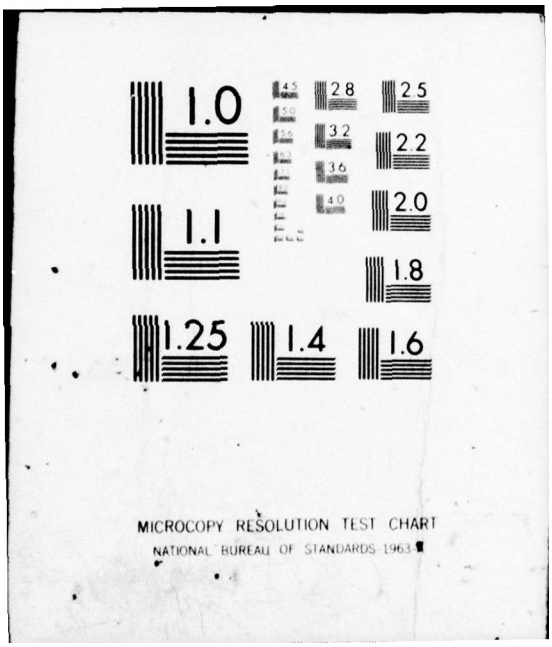
1.0
1.1
1.25
1.4
1.6
1.8
2.0
2.2
2.5
2.8
3.2
3.6
4.0
MICROCOPY RESOLUTION TEST CHART
NATIONAL BUREAU OF STANDARDS-1963

NORTHWESTERN UNIVERSITY

DEPARTMENT OF MATERIALS SCIENCE + Eng.

Technical Report, No. 14
February 10, 1977

Office of Naval Research
Contract N00014-75-C-0580
NR 031-733

EVALUATION OF PROCEDURES IN AUTOMATED RESIDUAL STRESS MEASUREMENTS.

by

M. R. James and J. B. Cohen

10 Feb 77

Distribution of this Document is Unlimited.

TR-14

83p.

EVANSTON, ILLINOIS 1473

EVALUATION OF PROCEDURES IN AUTOMATED RESIDUAL STRESS MEASUREMENTS

M. R. James and J. B. Cohen

Northwestern University

Evanston, Illinois 60201

ABSTRACT

The measurement of residual stress by the X-ray diffraction technique involves determining the lattice spacing of a crystallographic plane at different inclinations of the sample and relating the change in the spacing to a stress on the surface of the specimen. The sources of error in determining the residual stress are investigated in this report. A short review of the fundamental principles of the measurement is given. The important instrumental and geometric factors contributing to errors in the measured stress are presented. To account for random errors in the data accumulation on the measured stress, a complete statistical analysis based on a least-squares parabola is given.

Employing an automated diffractometer (see T.R. No. 16), an extensive investigation of the precision of the residual stress measurement was made to evaluate the various procedures offered in the literature to optimize the automation. The results indicate that a multiple least-squares parabola is the most reproducible method of defining the peak of the profile, in contrast to the common three point parabola used in the United States, the center of gravity used in Germany or the middle of the half-maximum intensity used in Japan. Also, for a standard diffractometer, the $\sin^2\psi$ technique is more precise than the usual two tilt method even

when the total time of analysis for each is identical. In studying various beam optic arrangements, it was found that the stationary slit (non-focusing method) offers the best system in that the measured stress is only mildly sensitive to sample displacement ($\sim$ 7 MPa for .25 mm displacement) and introduces very little instrumental broadening. The operational principles and use of a position sensitive detector (PSD) for the measurement of residual stress has been described previously (see T.R. No. 11). The PSD simultaneously collects data over the entire diffraction profile enabling the use of a multiple point parabola to define the peak without having to step scan the profile. Extensive testing is described which showed that this detector could achieve a speed of analysis heretofore never obtainable in the measurement of residual stress.

CHAPTER 1

The X-ray diffraction procedure for determining the surface residual stresses is well established.[4-7] Each family of identical planes of atoms in a polycrystalline material has a constant interplanar spacing, $d_{hk\ell}$ which, when acted upon by an elastic stress, changes to a new value dependent on the direction and magnitude of that stress. A change, $\Delta d_{hk\ell}$, in the interplanar spacing will cause a corresponding change, $\Delta\theta$, in the Bragg angle of diffraction by the family of planes. The strain, $\Delta d/d$, can be measured by the change in the diffraction angle and the stress can be obtained from the strain with formulae derived from linear isotropic elasticity theory.

The principal stresses σ_1 and σ_2, the surface stress, σ_φ, and the corresponding strain are shown in Fig. 1.1. The term ψ is the angle between the surface normal and the direction of strain being measured. Application of isotropic elasticity theory yields the following relationship between the principle stresses, surface stress and measured strain, $\varepsilon_{\varphi,\psi}$:[4]

$$\varepsilon_{\varphi,\psi} = \frac{1+\nu}{E}\sigma_\varphi \sin^2\psi - \frac{\nu}{E}(\sigma_1 + \sigma_2) = \frac{d_{\varphi,\psi} - d_o}{d_o} . \qquad (1.3)$$

In this equation, $d_{\varphi,\psi}$ is the lattice spacing in the direction defined by φ and ψ (see Fig. 1.1) and d_o is the interplanar spacing of the stress free state.

Equation 1.3 forms the basis of X-ray stress analysis and is utilized primarily in two methods; the '$\sin^2\psi$' and the 'two tilt' technique.

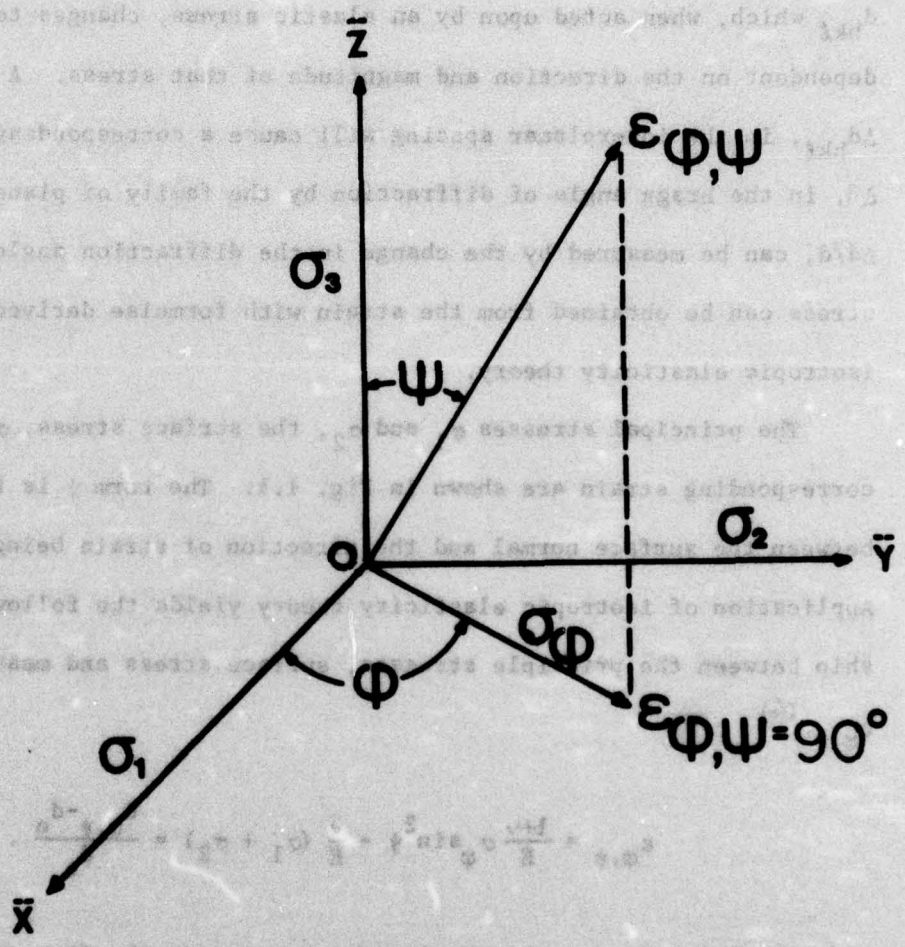

FIGURE 1.1 Illustration of the symbols used in X-ray stress measurement.

(A) '$\sin^2\psi$' Technique

In this method several values of lattice strain are measured, each at a different ψ tilt of the specimen. It is possible to determine any surface component of stress from a least-squares straight line for the lattice strain as a function of $\sin^2\psi$.

From Eq. 1.3:

$$\sigma_\varphi = \frac{m^*}{\left(\frac{1+\nu}{E}\right)} \qquad m^* = \frac{\partial\, \epsilon_{\varphi,\psi}}{\partial\, \sin^2\psi} \tag{1.4}$$

In terms of the interplanar spacing it follows that:

$$\sigma_\varphi = \frac{m'}{d_o\left(\frac{1+\nu}{E}\right)} \qquad m' = \frac{\partial\, d_{\varphi,\psi}}{\partial\, \sin^2\psi} \tag{1.5}$$

Because several values of d_φ are determined, errors resulting from random fluctuations of $d_{\varphi,\psi}$ are minimized. Four or six ψ tilts, taken in equal increments of $\sin^2\psi$, are normally utilized.

(B) 'Two Tilt' Technique

Isotropic elasticity theory predicts the strain $\epsilon_{\varphi,\psi}$ to be linearly dependent on $\sin^2\psi$, as in Eq. 1.3. When this holds true only two inclinations of the sample are necessary to determine the surface stress. The interplanar spacings are determined at $\psi=0$ and at an inclination of $\psi=\psi$. The formula relating the stress to the strain is then given by:[5]

$$\sigma_\varphi = \left(\frac{E}{1+\nu}\right) \cdot \frac{1}{\sin^2\psi} \cdot \frac{d_{\varphi,\psi} - d_o}{d_o} \,. \tag{1.6}$$

The term $(E/1+\nu)\cdot 1/\sin^2\psi$ is often combined into a calibration constant, K, which can be experimentally determined for a particular combination of ψ and reflecting planes in a given material. Experimental determination of K is desirable because bulk values of E and ν are not necessarily applicable.[6]

It is unfortunately common practice to replace $(d_{\varphi,\psi}-d_o)/d_o$ in Eq. 1.6 by the approximation $-\cot\theta\cdot\frac{1}{2}(2\theta_o-2\theta_\psi)$ on the basis of Bragg's law to obtain a formula in terms of the peak position 2θ:

$$\sigma_\varphi = \tfrac{1}{2}\cdot\frac{\pi}{180}\cdot\left(\frac{E}{1+\nu}\right)\cdot\frac{1}{\sin^2\psi}\cdot\cot\tfrac{1}{2}(\theta_o+\theta_\psi)\cdot(2\theta_o-2\theta_\psi) \qquad (1.7)$$

where $2\theta_o$ and $2\theta_\psi$ are in degrees. For small peak shifts this does not induce much error. The stress constant then becomes:

$$K = \frac{1}{2}\cdot\frac{\pi}{180}\cdot\left(\frac{E}{1+\nu}\right)\cdot\frac{1}{\sin^2\psi}\cdot\cot\tfrac{1}{2}(\theta_o+\theta_\psi) \qquad (1.8)$$

and

$$\sigma_\varphi = K\,\Delta 2\theta\ .$$

CHAPTER 2

The methods of residual stress measurement by X-ray diffraction just described are based on the fundamental equation (Eq. 1.3) derived by isotropic elasticity theory and assume homogeneous deformation. These methods have been shown to sometimes yield anomalous results when applied to samples which have been plastically deformed uniaxially in tension[18,19]

or by rolling.[19,20] The anomalous results are not true mechanical macrostresses and may be attributed to a number of causes.[11]

Recent work by Marion and Cohen[19] has led to the quantification of a deformation model to account for one of the anomalies in the X-ray technique of residual stress measurement which occurs after plastic deformation. The classical formulae around which all X-ray technique of residual stress analysis (Eq. 1.3) predicts a linear dependence of $d_{\phi,\psi}$ on $\sin^2\psi$. A non-linear dependence of the X-ray measured strain on $\sin^2\psi$ has been reported for a number of materials which have undergone plastic deformation due to elongation[21-22] or rolling.[10] Such deviations from the theory has prompted questions concerning the validity of the X-ray measurement in such cases. Marion and Cohen[19] attributed the non-linear dependence of d on $\sin^2\psi$ to the relief of microstrains in subgrain interiors which are oriented to be relieved by a dynamic recovery process proposed by Weidemann et al.[23,24] This produces a non-random distribution in the interplanar spacing which is related to the texture developed during the plastic deformation process. The authors developed a distribution function, $f(\psi)$, describing the variation in interplanar spacing at each ψ inclination, and incorporated the non-linear behavior of d vs. $\sin^2\psi$ into the general formulae for the X-ray method of residual stress analysis. By measuring both the interplanar spacing, $d_{\phi,\psi}$, and the distribution function, $f(\psi)$, as a function of $\sin^2\psi$, the non-linear dependence of d may be separated from the linear component through the following formula:

$$d_{\phi,\psi} = (d_{max}-d_\beta)f(\psi) + d_o\left(\frac{1+\nu}{E}\right)\sigma_\phi\sin^2\psi + d_\beta \,. \qquad (2.1)$$

The term d_{max} corresponds to the lattice spacing in a region that is fully relieved and d_β the lattice spacing in a region that has not relieved. The distribution function describes the variation of relief with orientation and is calculated by determining the texture in the region of the pole figure for which the residual lattice strain is measured. This is most easily accomplished by measuring the integrated intensity of the diffraction peak of interest at each ψ inclination and normalizing the distribution function by setting $f(\psi) = 1$ at the maximum value of the curve of integrated intensity. The correlation between the change in the distribution function and the oscillations in d vs. $\sin^2\psi$ is shown vividly in Fig. 1.3.

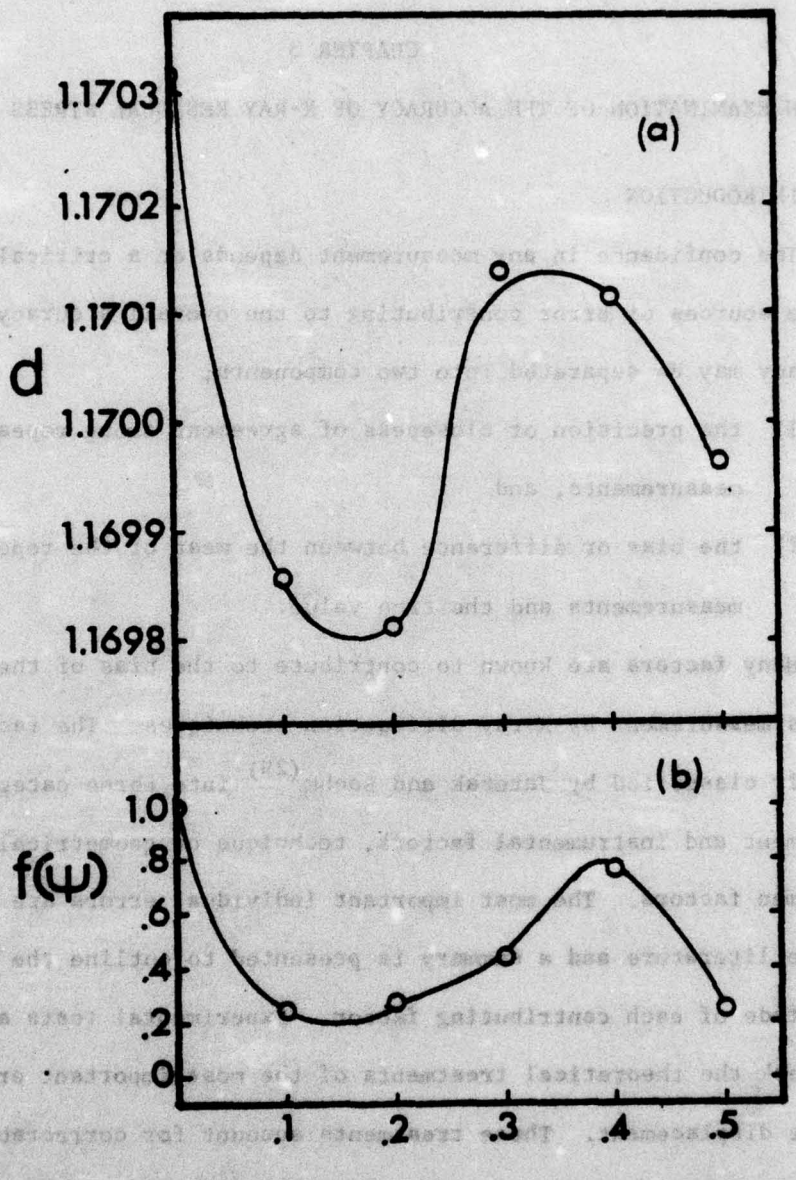

FIGURE 1.3 - from Marion[30]
a) d vs. $\sin^2\psi$ for Armco iron specimen; reduced 69 pct by rolling; 211 peak with CrK_α.
b) Texture for sample described in (a). $f(\psi)$ represents the normalized texture distribution function.

CHAPTER 3

AN EXAMINATION OF THE ACCURACY OF X-RAY RESIDUAL STRESS ANALYSIS

3.1 INTRODUCTION

The confidence in any measurement depends on a critical consideration of the sources of error contributing to the overall accuracy. The accuracy may be separated into two components;

1) the precision or closeness of agreement among repeated measurements, and
2) the bias or difference between the mean of the repeated measurements and the true value.

Many factors are known to contribute to the bias of the residual stress measurement by X-ray diffraction techniques. The factors are broadly classified by Jatezak and Boehm[29] into three categories, equipment and instrumental factors, technique or geometrical factors and specimen factors. The most important individual errors are well treated in the literature and a summary is presented to outline the source and magnitude of each contributing factor. Experimental tests are described to check the theoretical treatments of the most important error, that of sample displacement. These treatments account for correctable errors in the measurement but do not delineate the potential accuracy of the technique or apparatus.

The precision of the X-ray residual stress measurement relies on reproducible determination of the peak shift. Numerical methods of peak location are mandatory for fully computerized control of the measurement. The peak may be found by fitting a smooth curve to the experimental data.

Such a curve cannot give an absolute measure of the peak location as the data is subject to random errors. These random errors occur because the diffracted intensity is measured at a finite number of 2θ positions and every measurement is subject to a statistical counting error. Statistical treatments for different numerical methods for measuring line-profiles can be found in the literature. These include the centroid,[60,61] median[60,62] and geometrical peak.[63]* The peak position, located by a least squares parabola is shown here to be the most precise method. A statistical analysis based on the least-squares parabola is extended here to the determination of residual stress. The region of fit of a parabola to the diffraction profile is discussed. The commonly used three point parabolic fit is examined theoretically and experimentally. A test on the effect of the number of data points is made to determine if the three point fit is actually the optimum procedure for recording data. It is shown that for fixed total time of data accumulation, the observed precision from replicate tests is improved by using many data points, especially for broad profiles. The three point parabolic fit is adequate only for samples exhibiting a sharp profile.

The precision of the 'two tilt' and '$\sin^2\psi$' stress techniques are tested under identical conditions so that comparisons on the relative accuracy of each method can be made. The '$\sin^2\psi$' method is shown to have a greater precision that the 'two tilt' procedure when a fixed total time of data accumulation is used. In addition, the precision of

---

*Any consistent feature of the line profile may be utilized to define the reference point from which the position of the profile is based. Three common features in residual stress analysis are the centroid, midpoint of the half-intensity breadth value and the peak. The positions located by each method are not identical but must be reproducible. Comparisons of the reproducibility of each method are given in Sec. 3.3.2 and show that a least squares parabola exhibits the best reproducibility.

the residual stress measurement using a position sensitive detector is tested. Because many data points are obtained in the region of curve fitting, the PSD is shown to be a both rapid and precise means of accumulating the data. A least-squares parabola fit to the region of the peak of the diffraction profile obtained with the PSD is shown to be the most reproducible means of locating a reference position on the profile.

3.2 FACTORS INFLUENCING BIAS IN THE MEASUREMENT

There are three broad categories into which all factors influencing the bias can be classified: instrumental, geometrical, and specimen factors. A detailed list compiled by Jatezak and Boehm[29] is reproduced in Table 3.1.

Many of the sources of error are dependent on either the capability of the experimenter (alignment, sample position) or operating conditions (electronic stability) of the equipment and, as such, are unpredictable. An explanation of the predictable factors, their effects and correction terms are given below.

3.2.1 Angular Dependent Intensity Factors

(A) Lorentz-Polarization Factor

This term combines two 2θ dependent intensity corrections, the lorentz factor and the polarization factor, which arise from the geometry of the diffraction process.[33] The Lorentz factor for a powder can be considered as two independent factors, one arising from the number of particles in the sample which are in orientation to contribute to a particular reflection and the second arising from the fraction of the reflection ring which is detected. The first factor is independent

TABLE 3.1

FACTORS WHICH INFLUENCE ACCURACY AND PRECISION IN X-RAY STRESS MEASUREMENTS*

Equipment and Instrumental Factors	Technique and Geometrical Factors	Specimen and Material Factors
Alignment Technique	Selection of Radiation	Type of Material
Specimen Alignment Technique	Selection of (hkℓ) Plane	Crystal System
Availability of θ/2θ Goniometer Rotation	Selection of Apertures, etc.	Specimen Preparation Technique
Availability of Parafocusing	Beam Focusing Technique	Specimen Size
Available Apertures	Method of Correction for LP and Absorption Effects	Specimen Geometry
Available Soller Baffles	Counting Statistics	Elastic Constants
Detector Type	Scanning Procedure	Mass Absorption Coefficients
Availability Proper Radiation	Stress Calibration Technique	Grain Size
Noise Discrimination Circuit	Deviation from Plane Stress	Effect of 2nd Phase
Power Stability	Corrections for Beam Penetration	Type of Deformation Causing Stress
Electronic Stability	Corrections for Material Removal	Stacking Faults
Availability High KW Tubes		Twinning
		Texture

*From Jatczak and Boehm.[29]

of the detection geometry whereas the second factor is dependent on the acceptance function of the detector[64] and the velocity of the reflection through the Ewald sphere.[33] The polarization term arises because X-rays are polarized after being scattered or diffracted, the amount of polarization depending upon the angle through which it is scattered or diffracted. The conventional correction factor (combining the Lorentz and polarization factors) for filtered radiation and point counting, designated LP, is:[7]

$$LP = \frac{1 + \cos^2 2\theta}{\sin^2 \theta} \quad . \tag{3.1}$$

The measured intensity need only be divided by Eq. 3.1 prior to processing.

Cooper and Glasspool[64] have shown that in some cases, notably when the axial (perpendicular to the plane of the diffractometer) half-height of the detector aperature is large and the scattering angle becomes small ($\theta_B \rightarrow 0°$) or large ($\theta_B \rightarrow 90°$), the curvature of the diffraction cone becomes important. In the traditional derivation of the Lorentz factor, the curvature of the cone is ignored. For 2θ values greater than about 9° and less than 171° the conventional Lorentz factor is in error by less than 1%, as calculated by Cooper and Glasspool. This small error combined with the fact that in peak location measurements only the angular dependent changes in the correction factor are important make the conventional Lorentz factor quite satisfactory.

(B) Absorption Factor

The path length of the primary and diffracted X-rays within the specimen differ when the specimen is tilt by ψ. For a flat specimen the measured intensity is corrected for absorption by dividing by:[26]

$$ABS = 1 - \tan \psi \cot \theta \qquad (3.2)$$

The angle ψ is defined as positive when the normal to the sample moves towards the X-ray source. Although ψ is a polar angle, its sign must be known in order to calculate the correct absorption coefficient.

(C) Atomic Scattering Factor

The intensity of the diffracted beam depends in part on the square of the structure factor. The angular dependent part of this term, denoted the scattering factor f, should be accounted for by dividing the intensity by f^2. The atomic scattering factor is a function of the atoms comprising the crystal, the diffraction angle θ and the wavelength of the radiation and values are published in the International Tables for X-Ray Crystallography.(65)

(D) Temperature Factor

The Debye temperature factor is the reduction in intensity due to thermal motion of the lattice. Atoms in a crystal vibrate due to temperature so that at any instant corresponding atoms are not separated by exact multiples of cell dimensions. Scattering from two such atoms will not be exactly in phase resulting in a reduction in the structure factor. The correction for this reduction, called the temperature factor, is slightly dependent on sin θ and strictly speaking should be accounted for.

Over the range of 154°2θ to 158°2θ where the most commonly used peak for stress analysis of steel occurs with $Cr_{K\alpha}$ radiation, Short and

Kelly[28] calculated the change in the intensity factors. Their values are reproduced in Table 3.2 and indicate that the Debye temperature factor is very small in relation to the others. For generality, the Lorentz-polarization, absorption and scattering factors have been included in the automated residual stress analysis program developed in this study.

3.2.2 Factors for "Beam Optics"

Beam focusing depends on the geometric arrangement of the X-ray path and on the horizontal and vertical divergence of the beam. The important methods of 'beam optics' are discussed below.

(A) Variation of the Focal Point with θ and ψ

There are two methods of beam focusing used in X-ray stress measurement, the parafocusing method and the stationary method. An excellent study on the errors associated with each method is given by Zantopulos and Jatczak.[31]

In the parafocus technique the receiving slit and/or detector are moved along a radius of the goniometer toward the specimen to fulfill the changing beam focusing condition when the inclination, ψ, of the specimen is varied.[26]

The distance from the sample to the focus position is given by:[7]

$$R_p' = R_{GC} \frac{\cos(\psi + (90-\theta))}{\cos(\psi - (90-\theta))} \qquad (3.3)$$

where R_{GC} is the goniometer radius.

In the stationary method the receiving slit and detector remain on the goniometer circle at all times thereby deliberately not fulfilling

TABLE 3.2

CHANGE IN CORRECTION FACTORS FROM 154° TO 158° 2θ
FOR Fe AND CrK_α RADIATION*

Factor	154° 2θ	158° 2θ	Change
Lorentz ($1/\sin^2\theta$)	1.0533	1.0378	- 1.47%
Polarization ($1+\cos^2 2\theta$)	1.8078	1.8596	+ 2.87%
Absorption ($\psi = 0°$)	1.	1.	0
Absorption ($\psi = 45°$)	0.7691	0.8056	+ 4.74%
Atomic Scattering (f^2)	1.3503	1.3322	- 1.34%
Temperature	0.8653	0.8634	- 0.22%

*From Short and Kelly.[28]

focusing conditions. A sacrifice in intensity is made but the complication of moving the receiving slit and/or detector is avoided. The Japanese use a version of this technique described as the parallel beam method.[29] Using long Soller baffles or plates perpendicular to the diffractometer plane rather than in the usual horizontal position, the X-rays are made to be highly collimated parallel beams which do not have a focal point. The angle of diffraction is uniquely defined by the angle between the primary and diffracted beam (see Fig. 3.1) and as such a receiving slit is not necessary.

(B) Horizontal Beam Divergence

In the parafocusing method, true focus demands that the sample surface lie on the focusing circle which is given by:[7]

$$R_{FC} = R_{GC}/2 \sin (\theta + \psi) \qquad (3.4)$$

True focusing demands a continuous change in the curvature of the specimen during θ and ψ angular movements. Since this is generally not practical an error will arise which is dependent on the curvature of the sample and the horizontal beam divergence. Marion[30] has derived a simple formula to estimate the error in the peak shift due to beam divergence. Defining α as half the angular beam divergence the peak shift in degrees 2θ, $\delta(\Delta 2\theta)_{BD}$, between the $\psi = 0°$ and $\psi = \psi°$ inclination is:

$$\delta(\Delta 2\theta_{BD}) = \Delta 2\theta)_{\psi=0} - \Delta 2\theta)_{\psi=\psi} \qquad (3.5)$$

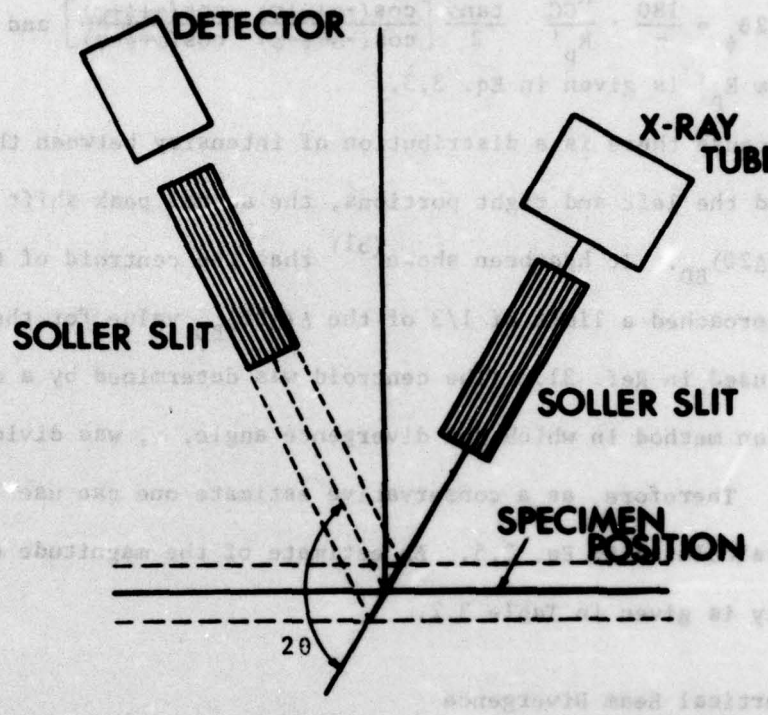

FIGURE 3.1 Illustration of parallel beam geometry. The angle 2θ is uniquely defined by the angular relationship between the two sets of soller slits and is independent of the sample position. The dashed lines represent other sample positions that would not affect the angle of diffraction.

where $\Delta 2\theta_{\psi} = \frac{180}{\pi} \cdot \frac{R_{GC}}{R_p'} \cdot \frac{\tan\alpha}{2} \left[\frac{\cos(-\alpha+\psi+\varphi)}{\cos(-\alpha+\psi-\varphi)} - \frac{\cos(\alpha+\psi+\varphi)}{\cos(\alpha+\psi-\varphi)} \right]$ and $\varphi = 90 - \theta$. The term R_p' is given in Eq. 3.3.

Because there is a distribution of intensity between the central beam and the left and right portions, the actual peak shift will be less than $\delta(\Delta 2\theta)_{BD}$. It has been shown[31] that the centroid of the diffracted beam approached a limit of 1/3 of the $\delta(\Delta 2\theta)_{BD}$ value for the ψ, α and 2θ values used in Ref. 31. (The centroid was determined by a computer iteration method in which the divergence angle, α, was divided into 1000 parts). Therefore, as a conservative estimate one can use 1/2 of the value calculated in Eq. 3.5. An estimate of the magnitude of this quantity is given in Table 3.2.

(C) Vertical Beam Divergence

Grains that have planes slightly tilted from that of the diffracting position for a parallel incident beam may contribute weakly to a peak giving rise to an apparent peak shift. This has been thoroughly treated by Cohen.[66] The peak shift depends on the amount of texturing and the slit system and is difficult to determine exactly but is quite small. An estimate is given in Table 3.2.

In the parafocusing and stationary slit techniques systematic errors are produced by focusing aberrations during diffraction due to imperfect specimen contours and beam divergence as shown in Fig. 3.2. The photon rays are in a divergent beam and diffract from a sample which is not curved to the focusing circle so that the point of focus in Fig. 3.2,

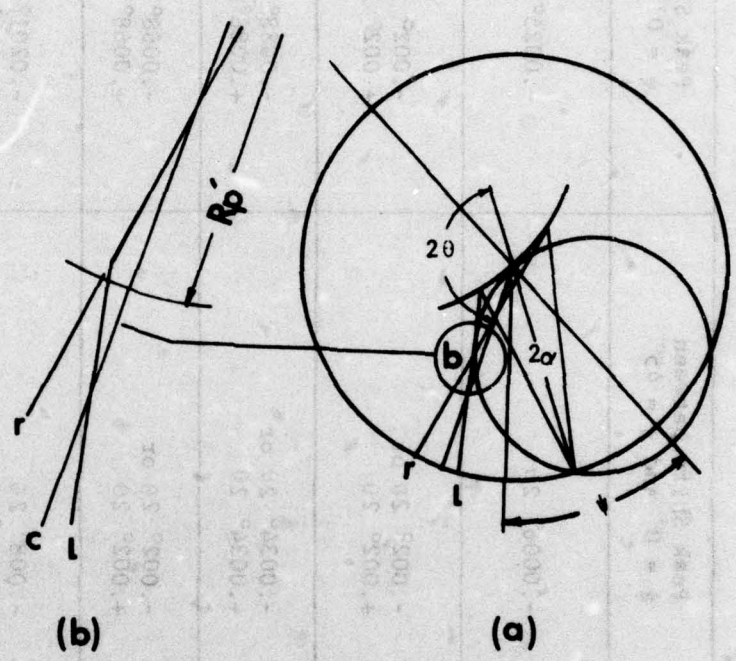

FIGURE 3.2 Departure from ideal focusing condition. The intersection of the left, L, right, R, and center, C, rays are shown in b. The focus is not a point for a sample with non-ideal curvature.

TABLE 3.2

TYPICAL INSTRUMENTAL ERRORS IN PEAK LOCATION FOR $2\theta = 156°$
(Approximately the 211 CrK_α Peak from Iron)

Cause	Peak Shift between $\psi = 0°$ and $\psi = 45°$	Peak Shift between $\psi = 0°$ and $\psi = 60°$
Horizontal beam divergence ($\alpha = .5°$) (Taking 1/2 $(\delta(\Delta 2\theta)_{BD})$ see text	-.0006° 2θ	-.0025° 2θ
Vertical beam divergence (Assuming strong texture using divergent Soller slit, no receiving Soller slit)	-.002° 2θ or +.002° 2θ	-.002° 2θ or +.002° 2θ
Sample displacement $\Delta x = \pm .025$ mm	-.0034° 2θ or +.0034° 2θ	-.0088° 2θ or +.0088° 2θ
ψ-axis displacement $\Delta x' = \pm .025$ mm	-.002° 2θ or +.002° 2θ	-.0068° 2θ or +.0068° 2θ
Maximum total errors† a) in - 2θ direction b) in + 2θ direction	-.008° 2θ +.0068° 2θ	-.0201° 2θ +.0149° 2θ
Maximum error in stress for steel*	-4.74 MPa (-690 psi) or +4.0 MPa (-585 psi)	-7.0 MPa (-1150 psi) or +5.9 MPa (+860 psi)

†Note: Maximum error is either one of these but not the total range.

*Calculated for steel from $\sigma_\phi = K_\psi (2\theta_\perp - 2\theta_\psi)$ where $K_{45} = 593$ MPa/°2θ and $K_{60} = 396$ MPa/°2θ.

is not really a point but simply a converging area for the beam which causes a focusing aberration. Zantopulos and Jatczak[31] studied these systematic errors by analytically describing the beam path for any particular ray within the divergent beam from the source to the detector. By dividing the divergent beam into 1000 such rays they calculated the centroid of the rays at the detector for both 'beam optic' techniques using specimens of varying curvature. They concluded the focusing error due to imperfect specimen contour and horizontal beam divergence for the stationary slit method yields about one third the error of the para-focusing method at $2\theta = 156°$; the discrepancy increasing for smaller 2θ. In addition, the error when using a beam divergence of 1° on flat samples or samples having reasonable curvature, will be less than 16 MPa (2.3 ksi).

One factor not included in the analysis by Zantopulos and Jatczak is the ability to accurately position the receiving slit when the para-focusing technique is used. The exact position along the radius is not critical because, as shown above, the focus is not actually a point but an area of convergence of the rays. The critical positioning comes about in moving the receiving slit <u>exactly</u> <u>along</u> the radius. Any deviation will cause an apparent peak shift because the angular relationship between the direct beam ($0°2\theta$) and the receiving slit changes.

Using an automated receiving slit bracket and an automated residual stress program* replicate measurements were carried with and without receiving slit movement on a 1045-1 sample which had a reasonably sharp 211 diffraction profile. Using $Cr_{K\alpha}$ radiation, 15 repeated measurements were made using a three point parabolic fit to define the diffraction peak and a

*The automated residual stress program is described in Chapter 4.

statistical counting accuracy of ± 1.72 MPa (± 250 psi) an average value for the stress of -164.1 MPa (-23790 psi) for the parafocusing geometry and -169.8 MPa (-24636 psi) for the stationary slit method was obtained. While the results are remarkably similar, the observed error of one standard deviation from the mean value was ± 3.6 MPa (± 520 psi) and ± 7.4 MPa (± 1080 psi) for the stationary slit and parafocusing geometries respectively. The repositioning of the receiving slit was very accurate and introduced only a small random error of about ± 4 MPa (± 600 psi). The bracket uses a worm gear and dovetail slide to move the receiving slit and is considered very sturdy. Other, less perfect systems such as manually repositioning the slit, are likely to cause larger random errors in the measurement.

The effect of systematic errors for the parallel beam method has been studied by Fukura and Fujirwara[67] and Aoyma.[68] The advantage of this method is that errors due to sample displacement are minimized enabling simple sample alignment. However, there are several points that are not yet clear. The intensity provided by the parallel beam method is less than with the focusing methods and instrumental broadening is greater which could combine to decrease the precision of the method. These points are examined experimentally in Sec. 3.8.

3.2.3 Instrumental Errors

(A) Sample Displacement

The largest single source of error is displacement of the sample. If the effective diffracting volume is not located at the center of the diffraction circle, there is a relative shift between $\psi=0^\circ$ and $\psi=\psi^\circ$ as

seen in Fig. 3.3. This has been treated by Cohen[66] and French[69] who derive a formula to calculate the peak shift. Denoting ΔX as the displacement, the equation for the error in peak shift at two tilts in degrees 2θ is:

$$\delta(\Delta 2\theta)_{SD} = \frac{360}{\pi} \Delta X \cos\theta \left[\frac{1}{R_{GC}} - \frac{\sin\theta}{R_p' \sin(\theta+\psi)}\right] \qquad (3.6)$$

where R_p' is given in Eq. 3.3 and R_{GC} is the goniometer radius. The peak shift due to sample displacement has been experimentally measured in this study (see Sec. 3.7) verifying Eq. 3.6 for the parafocusing and stationary techniques.

Cohen[66] suggests a simple and precise method to check for sample displacement on a diffractometer. For cubic structures Cohen showed:

$$\frac{a_{hk\ell} - a_o}{a_o} = -\frac{\Delta X}{R_{GC}} \frac{\cos^2\theta}{\sin\theta} \qquad (3.7)$$

where a_o is the extrapolated lattice parameter, $a_{hk\ell}$ the lattice parameter at a peak $hk\ell$, ΔX the displacement of the sample off the true center of the diffractometer and R_{GC} the radius of the goniometer circle. From a plot of $a_{hk\ell}$ vs. $\frac{\cos^2\theta}{\sin\theta}$ the slope equal to $-a_o\Delta X/R_{GC}$ can be obtained and the displacement calculated. A positive slope means the sample is displaced too far back (i.e., towards the back surface of the sample). One must only determine the angle of three or more Bragg peaks and form a plot of $a_{hk\ell}$ versus the function $\cos^2\theta/\sin\theta$. This method of alignment is incorporated in the automated residual stress program used in this study; a sub-program of the package automatically determines the peak positions and calculates the displacement, ΔX, and repositions the sample.

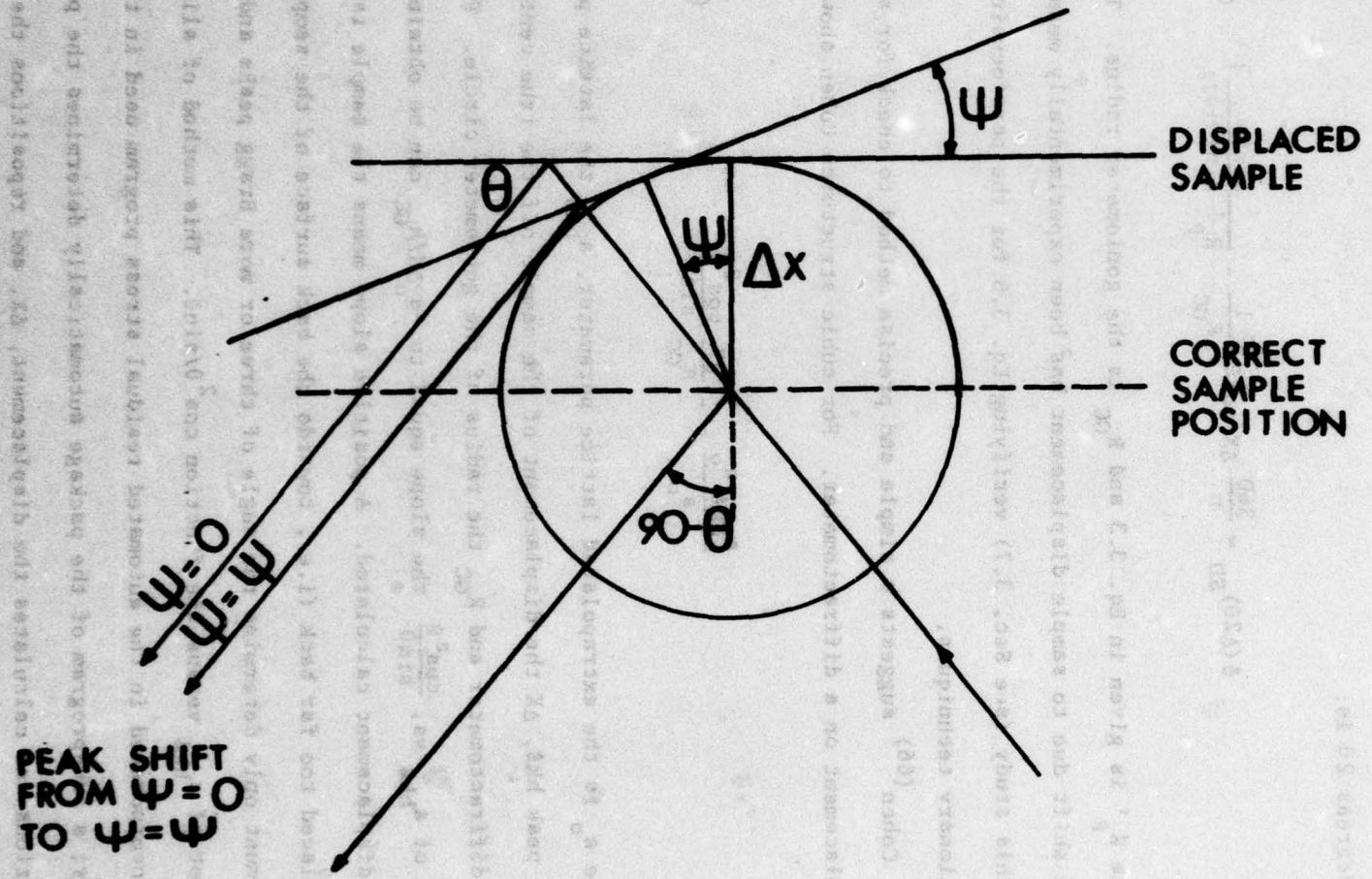

FIGURE 3.3 Illustration of the effect of sample displacement on the peak position when the sample is rotated ψ degrees.

(B) Effect of ψ Axis Missetting

The axis of inclination of the sample, ψ, must be coincident with the 2θ axis or a peak shift will result as shown in Fig. 3.4. Marion[30] has derived this error and calculates the peak shift in degrees 2θ to be:

$$\delta(2\theta)_{\psi A} \simeq \frac{-360}{\pi} \Delta X' \frac{\sin\theta \cos\theta (1-\cos\psi)}{R_p' \sin(\theta+\psi)} \qquad (3.8)$$

where $\Delta X'$ is the effective displacement. This source of error can be important on diffractometers employing an attachment to give the ψ rotation. On the Picker diffractometer the 2θ and ω axis rotate about the same shaft so no missetting is possible. However, the φ axis of a G.E. χ-circle was also utilized occasionally. The missetting of the φ axis with respect to the 2θ axis was measured* to be .05 mm giving an effective peak shift of $.005°2\theta$ for a 45° tilt (approximately 3 MPa (435 psi) for Fe).

An estimation of the systematic error is calculated in the automated residual stress program. This includes the error due to horizontal beam divergence, sample displacement and ψ axis missetting, which are the three major errors (see Table 3.2).

3.3 METHOD OF PROFILE LOCATION

3.3.1 Introduction

Any consistent feature of the line profile may be utilized to define a reference point from which the position of the profile is based.

---

*By mounting a sample on the χ-circle, both the φ axis of the χ circle or the ω axis of the Picker diffractometer could be used to accomplish the ψ tilt. The missetting of the χ circle was obtained by comparing the peak position after rotating the sample using each axis for the tilt.

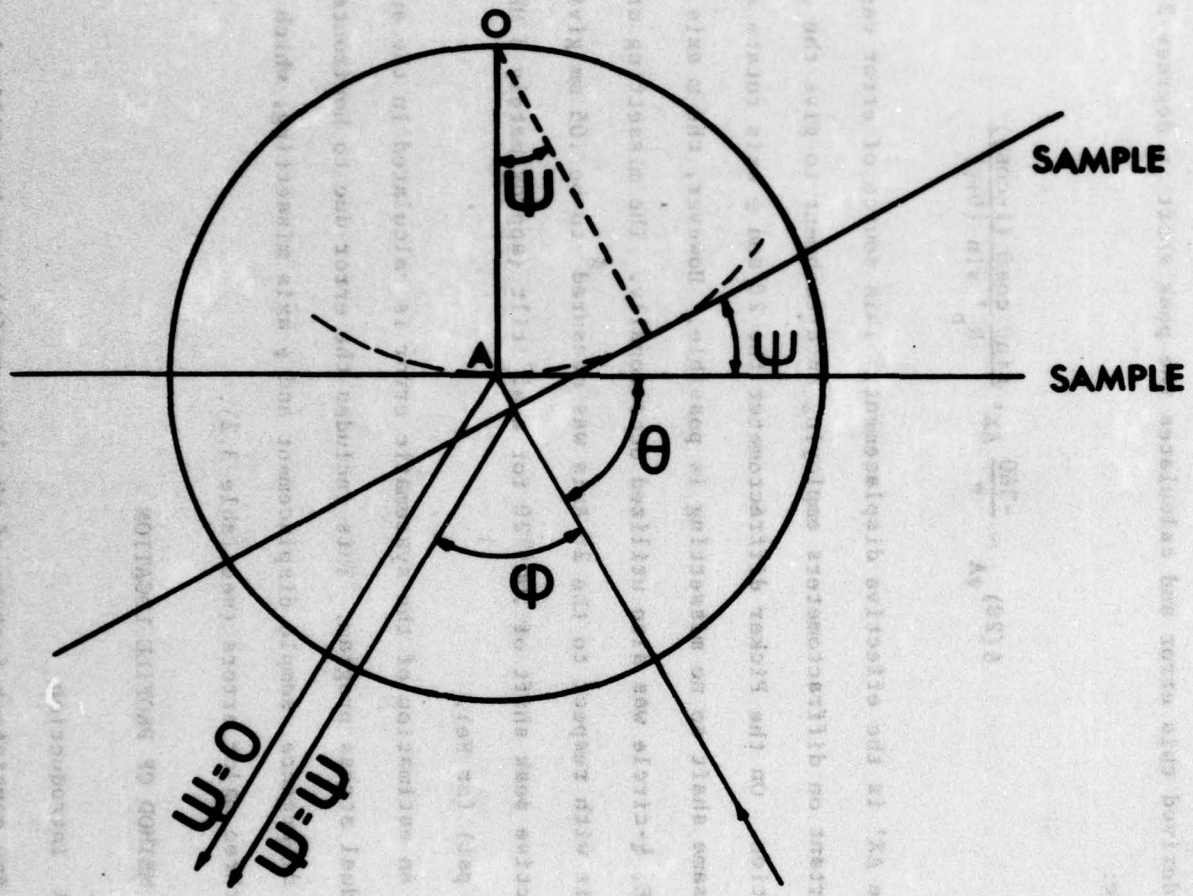

FIGURE 3.4 Illustration of the effect of ψ rotation axis not corresponding to the 2θ axis (point A is the axis of 2θ and point O is the axis of ψ).

The position located by any such method need not correspond with that defined by any other as long as the reproducibility is sufficient for the measurement. In residual stress measurements using X-ray diffraction, the profile has been traditionally defined in the U.S. by the apex of a parabola fit to the top region of the curve. Qualitatively, this gives equal weight to all observed data points to define the peak location. It has been suggested[70] that the center of gravity or centroid gives a more reproducible location of the peak, however, data was given only for the 422 peak of an annealed gold powder which is a well defined peak having a good peak to background ratio. In Japan, the half-value breadth and quarter-value breadth[71] method are the adopted feature to represent the profile position. These involve using the midpoint of a chord drawn through the profile at a particular height. These three methods, the peak, centroid and half-value breadth are compared for reproducibility in Sec. 3.3.2. The peak is shown to be the most reproducible because the background does not need to be determined since only data near the peak and not across the whole profile is used. This implies that some method must be used to define the region of parabolic fitting and two such methods are compared in Sec. 3.3.3. The formulae for a least-squares parabola is derived in Sec. 3.3.4.

3.3.2 Comparison of the Precision of Various Measures of Profile Location

For the X-ray stress measurement, the determination of the diffraction angle by any reference point on the profile is sufficient because the calculation of stress is based only on the relative change of the diffraction angle. The precision of the centroid, half-value breadth and

peak* positions are compared using a position sensitive detector (PSD) to collect the data (see Sec. 2.5). The PSD system collects data across the entire diffraction profile simultaneously so that the data for any reference position can be obtained in the same time as for any other method.

In the half-value breadth method shown in Fig. 3.5, the diffraction angle of the relevant point is determined by the mean of two angles given by:

$$S_o = \tfrac{1}{2}(X_{-\frac{1}{2}} + X_{+\frac{1}{2}}) \qquad (3.9)$$

where $X_{\pm\frac{1}{2}}$ is the intersection of the profile curve and the straight line parallel to the background at half of the peak intensity (excluding the background).

The centroid or center of gravity of a diffraction profile is defined as:[74]

$$\langle 2\theta \rangle = \frac{\int 2\theta\, I(2\theta)\, d2\theta}{\int I(2\theta)\, d2\theta} \qquad (3.10)$$

Baucum and Ammons[70] suggest the centroid can be located with better precision than the peak position of the profile, although they did not make a direct comparison. The method of centroid calculation given by Baucum and Ammons is based on Simpson's rule for a parabolic approximation to the area under a curve. Referring to Fig. 3.6, the centroid, denoted

---

*The peak may be defined using a Cauchy profile,[72] Gaussian distribution,[73] 2nd, 3rd or 4th order polynomials[29] or a parabola.[26] The parabola was chosen to define the peak because it has such general acceptance[7] for stress measurements.

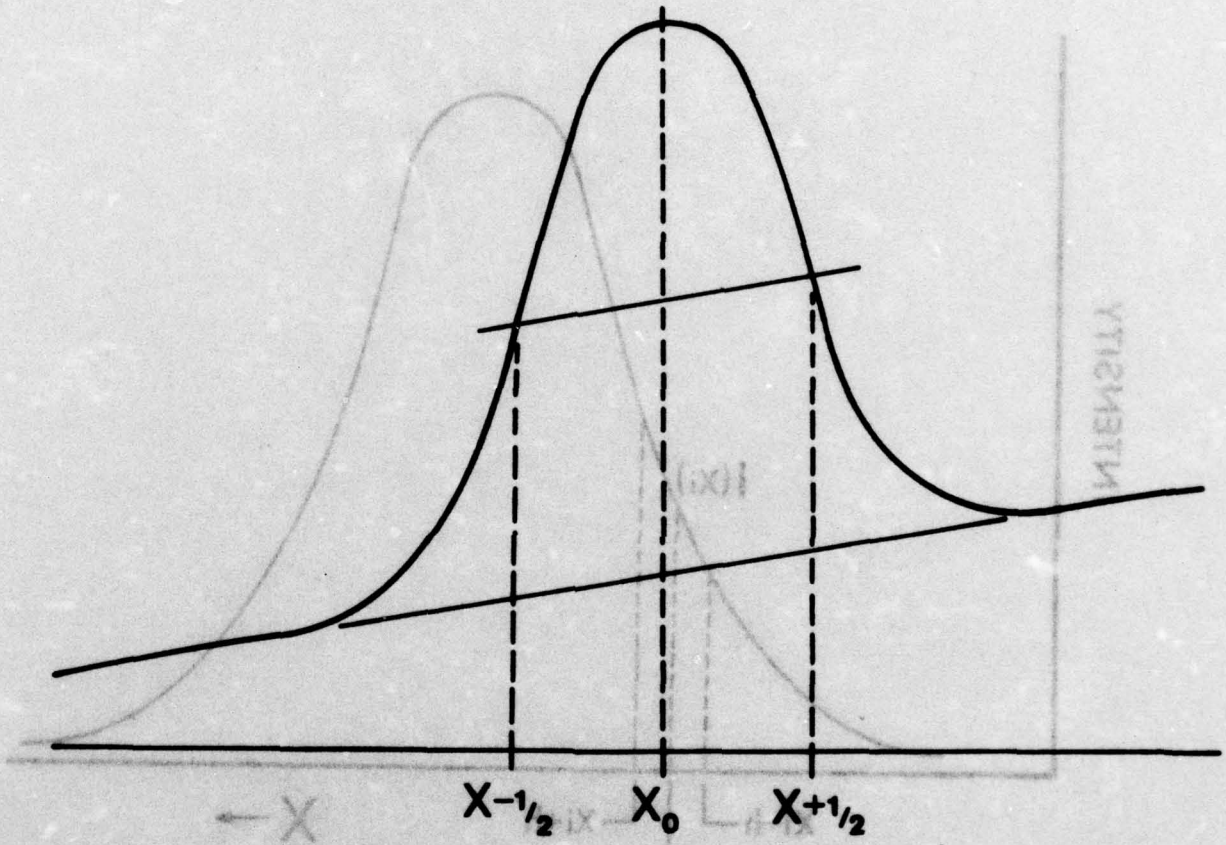

FIGURE 3.5 Calculation of half-value breadth.

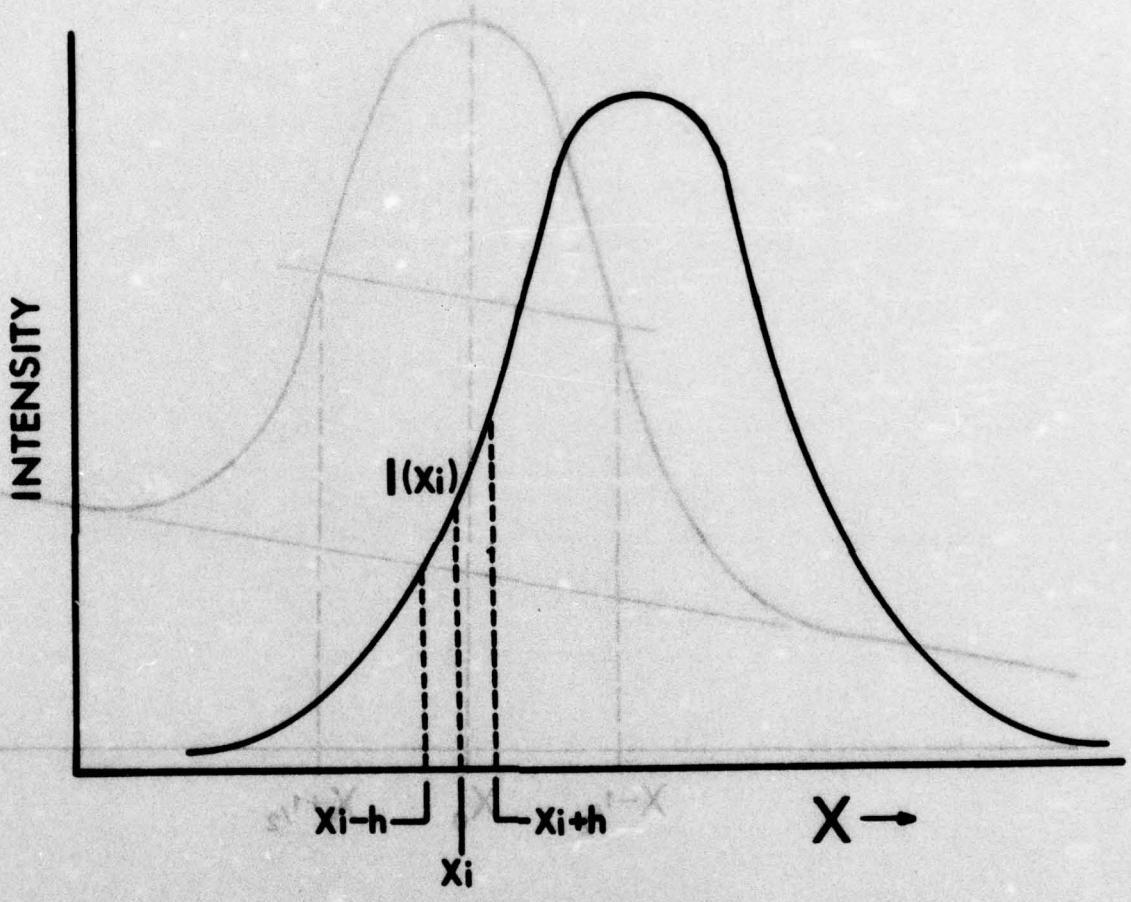

FIGURE 3.6 Centroid calculation

$\bar{X}$ is:

$$\bar{X} = \frac{\sum_{i=1}^{k} M_i}{\sum_{i=1}^{k} A_i} \tag{3.11}$$

where $A_i = \int_{X_i-h}^{X_i+h} I(X)dX \simeq \frac{h}{3}\left[I(X_i-h)+4I(X_i)+I(X_i+h)\right]$

and $M_i = \int_{X_i-h}^{X_i+h} XI(X)dX \simeq \frac{h}{3}\left[(X_i-h)I(X_i-k)+4X_iI(X_i)+(X_i+h)I(X_i+h)\right]$.

h represents the increment between data points and

$$k = \frac{\text{(no. data points)}-3}{2} + 1 \tag{3.12}$$

since three data points are required for the first increment and two for the rest.

Comparisons of the reproducibility of the least-squares parabola (see Sec. 3.3.4 for the formula), half-value breadth and centroid were made on the 1090-1 and 1045-2 samples using the CrKα 211 peak. The automated residual stress program described later for the PSD was modified to include the calculations required in Eq. 3.9 for the half-value breadth and Eq. 3.11 for the centroid. A linear background was determined by fitting a straight line through 50 data points, 25 on each side of the tails of the diffraction profile. The intensity corrections (Lorentz-polarization and absorption) were made after the background had been subtracted and prior to determining the centroid

and position of the half-value breadth. The least-squares parabola was fit to the top 15 pct of the profile without first subtracting the background.

The results of the ten replicate measurements are given in Table 3.3. The two-theta position represents the average calculated value over the ten measurements with one standard deviation from the mean being given in parenthesis. For the 1090-1 sample, having a sharp diffraction profile and low background, the centroid actually has a smaller variance than either of the other two methods. For the 1045-2 sample which has a poor peak to background ratio, the parabola has the lowest variance. For both samples, the half-value breadth gave the poorest reproducibility.

In X-ray residual stress measurements the peak to background ratio is usually poor, especially for hardened materials. In the centroid and half-value breadth reference points, the value is obtained from a truncated portion of the profile determined by the background subtraction. Thus, the background subtraction introduces an error (often referred to as the truncation error[62]). For the least-squares parabola, even if background is subtracted in determining the region of curve fitting (necessary only when a few data points are obtained, see Sec. 3.6.3) it does not affect the precision because the entire profile is not used minimizing the truncation error.

3.3.3 Region of Parabolic Fit

The region in the vicinity of the peak that can be used for the parabolic fit is not well defined. If it is assumed the true profile can be fit by a quasi-Lorentztian function (which is now becoming quite

TABLE 3.3

PRECISION OF VARIOUS MEASURES OF PROFILE POSITION
(10 measurements)

	Time (sec)	FWHM* (°2θ)	Half-Value Breadth (°2θ)	Centroid (°2θ)	Parabola (°2θ)
1090-1	50	.45	156.149 (± .021)**	156.096 (± .011)	156.186 (± .016)
1045-2	100	3.45	155.336 (± .064)	155.396 (± .085)	155.413 (± .020)

*FWHM is the full width at half of the maximum intensity.

**The term in ( ) represents one standard deviation from the average position over the 10 measurements.

popular in profile fitting powder patterns for structure analysis[75]), Thomsen and Yap[62] have shown that a parabola is valid for V less than .32 where:

$$V = \frac{2(2\theta_p - 2\theta_{min})}{W} \quad . \tag{3.12}$$

Here W is the full width at half maximum height of the diffraction profile, the peak position is $2\theta_p$ and the minimum value of 2θ lying on the parabolic curve is $2\theta_{min}$. While being theoretically justified Eq. 3.12 still depends on the profile being symmetric about the peak.

Koistinen and Marburger[26] suggest that data points for the parabolic fitting should be chosen which have intensities at least 85% of the maximum intensity. This rule has gained wide acceptance in X-ray residual stress analysis although it is purely empirical.

The'top 15 pct' rule is commonly used in X-ray residual stress analysis because it is simple to apply. Only data near the top region of the peak need be recorded and processed. The formula given by Thomsen and Yap requires knowledge of the breadth of the peak at half maximum intensity which demands accumulating data across the entire profile and determining the background.

The two rules for judging the region of the parabolic fit have been applied to experimental data. Table 3.4 tabulates the peak determined from a three point parabolic fit in column 4 and the minimum 2θ setting to be on a parabola, as calculated by each method in the next two columns. Column 2 is the full width at half the maximum intensity while column 3 records the ratio of the peak intensity to the background intensity.

TABLE 3.4

REGION OF PARABOLIC FIT FOR THE 211 DIFFRACTION PEAK FROM VARIOUS CRITERIA

Steel Specimen	FWHM* °2θ	Peak/Background Ratio	2θ Peak °2θ	2θ min Eq. 3.12 (°2θ)	2θ min '15% rule' (°2θ)	2θ min 15% rule After Background Subtraction (°2θ)
1090-1	.45	60	156.14	156.07	156.05	156.05
1045-1	1.5	3.5	155.89	155.65	155.61	155.65
1045-3	3.4	2.0	155.53	154.99	154.76	154.93
1045-2	5.1	2.6	155.50	154.68	153.20	154.40
1090-2	6.0	1.3	155.46	154.50	152.67	154.16
TBA G-5	5.8	1.3	155.29	154.33	152.69	154.29

*FWHM is the full width at half the maximum intensity.

For the first two samples listed, both having reasonably sharp diffraction profiles, the 'top 15 pct' rule of Koistinen and Marburger corresponds well with that of Eq. 3.12. This simularity breaks down as the profile becomes broader, as depicted by the remaining four samples. For these samples exhibiting increasingly broader diffraction profiles, the decreasing similarity between the 'top 15 pct' rule and Eq. 3.12 corresponds to a decreasing peak to background ratio (column 3). The background was not subtracted in determining the top 15 pct region resulting in the region being substantially larger. If a linear background is subtracted before applying the '15 pct' rule, the regions correspond quite closely, as seen in column 7. This background correction need not be exact. A quick estimate of the background obtained at one 2θ position away from the peak is sufficient since this is only concerned with determining the region of curve fitting. This procedure is incorporated in the computer program STRESS described in Chapter 4.

3.3.4 Derivation of Peak Location using Parabolic Fit

It is assumed that the data is obtained at an odd number of observation points and is also taken in equal increments of 2θ.* The data can then be said to be measured at 2n+1 points, the center point being taken as a working origin. The data accumulated at each jth point is I_j, the power in counts per second. If the 2θ increment between data points is designated as δ, the parabola is defined by:

$$a + b\delta j + c\delta^2 j^2 = I_j \qquad (3.13)$$

*Data taken using the PSD is in equal increments of distance which does not translate exactly into equal 2θ increments. The error in using a linear calibration constant to transfer distance along the PSD into °2θ is minimal for residual stress measurements (see Sec. 2.5.5).

and the least-squares solution is found by minimizing:

$$S = \sum_{j=-n}^{n} (a + b\delta j + c\delta^2 j^2 - I_j)^2 \qquad (3.14)$$

with respect to the unknown parameters a, b, and c. To solve Eq. 3.14, the partial derivatives of S with respect to each parameter are set equal to zero. This gives three equations for estimating the values of a, b, and c to minimize S.

For example:

$$\frac{dS}{da} = 0 = 2 \sum_{j=-n}^{n} (a + b\delta j + c\delta^2 j^2 - I_j) \qquad (3.15)$$

$$= a \sum_{j=-n}^{n} j^0 + b\delta \sum_{j=-n}^{n} j + c\delta^2 \sum_{j=-n}^{n} j^2 - \sum_{j=-n}^{n} I_j$$

$$= n_o a + 0 + n_2 \delta^2 c - \delta^{-1} M_o$$

where $n_i = \sum_{j=-n}^{n} j^i$ and $M_i = \delta^{i+1} \sum_{j=-n}^{n} j^i I_j$. The term M_i will be referred to as the i^{th} moment of the observed line profile.

Continuing in this manner the set of equations are:

$$n_o a + 0 + n_2 \delta^2 c - \delta^{-1} M_o = 0$$

$$0 + n_2 \delta b + 0 - \delta^{-2} M_1 = 0$$

$$n_2 a + 0 + n_4 \delta^2 c - \delta^{-3} M_2 = 0$$

Direct successive substitution for the three unknown parameters yields:

$$a = (M_o n_4 \delta^2 - M_2 n_2)/(n_o n_4 - n_2^2)\delta^3$$

$$b = M_1/\delta^3 n_2$$

$$c = (n_2 \delta^2 M_o - M_2 n_o)/\delta^5 (n_2^2 - n_o n_4)$$

The apex of the parabola is given by $\frac{dI_j}{d(\delta j)} = 0$, therefore

$$2\theta_p = 2\theta_o - b/2c \qquad (3.16)$$

where $2\theta_o$ is the working origin, that is, the 2θ position corresponding to the n=0 data point. From Eq. 3.16:

$$2\theta_p = 2\theta_o - (n_2^2 - n_o n_4)\delta^2 M_1/2n_2(n_2\delta^2 M_o - n_o M_2) \qquad (3.17)$$

(Angular dependent intensity corrections must be performed on the raw data before determining this peak position.)

3.4 STATISTICAL COUNTING ERROR IN PEAK LOCATION

3.4.1 Introduction

A simple mathematical expression (Eq. 3.17) has been derived to relate the measured intensities to the diffraction angle as given by the peak of the diffraction profile. There will be a statistical error in the calculated diffraction angle due to the finite number of X-ray quanta counted.

Wilson[63] has derived the statistical variance for a least-squares parabola fitted to data on X-ray peaks collected for fixed time at each observation point. Wilson's work is extended here to include both fixed time and fixed count methods of data collection to obtain the counting statistical error in a peak location. Propagation of this error to the error in the calculated stress is presented for both the '$\sin^2\psi$' and 'two tilt' methods of X-ray residual stress measurement in Sec. 3.5.

3.4.2 Derivation of Statistical Variance in the Peak Location

The variance of a general function, X, of several variables, $X=f(x_1,x_2,\ldots,x_n)$ is:[76]

$$V(X) = \left(\frac{dX}{dx_1}\right)^2 V(x_1) + \left(\frac{dX}{dx_2}\right)^2 V(x_2)+\ldots+2\left(\frac{dX}{dx_1}\,\frac{dX}{dx_2}\right)COV(x_1x_2)+\ldots \tag{3.18}$$

+ higher order differential terms. Here V(X) is the variance of X and $COV(x_i,x_j)$ is the covariance between variables x_i and x_j. Neglecting the higher differentials this can be rewritten as:

$$V(X) = \sum_{i,j}\left(\frac{dX}{dx_i}\,\frac{dX}{dx_j}\right) COV(x_ix_j) \tag{3.19}$$

If the function is linear, $X = \sum_i a_ix_i$, the standard error is given by:

$$V(X) = \sum_i a_i^2 V(x_i) \tag{3.20}$$

Since the count rate, $I_j \equiv x_j$ is a random variable having a finite variance, all quantities obtained by manipulating it also have a finite variance. Since the measured intensities are statistically independent:

$$\begin{aligned} COV(x_i,x_j) &= 0 \quad \text{for } i \neq j \\ COV(x_i,x_j) &= V(x_i) \quad \text{for } i = j \end{aligned} \tag{3.21}$$

Eq. 3.19 then becomes:

$$V(X) = \sum_j \left(\frac{dX}{dx_j}\right)^2 V(x_j) \ . \tag{3.22}$$

This equation is reasonably accurate for any nonlinear function providing the standard deviation of each variate is small, say 20% of the mean.[76]

Applying Eq. 3.22 to Eq. 3.17 and substituting for x_i the counting rate, I_j:

$$V(2\theta_p) = \sum_j \left(\frac{d2\theta_p}{dI_j}\right)^2 V(I_j). \tag{3.23}$$

The variance of the peak is dependent on the variance of the count rate, I_j, which depends on how the data is accumulated. The two common methods of determining the counting rate at the diffractometer setting $2\theta_j$ are the fixed time and fixed count techniques. Defining t_j as the time of data accumulation and C_j as the accumulated counts:

$$\begin{aligned} I_j &= C_j/t \quad \text{for fixed time} \\ I_j &= C/t_j \quad \text{for fixed counts} \end{aligned} \tag{3.24}$$

The variance (denoted hereafter as $\sigma^2(\ )$, the standard deviation squared) of the count rate is derived by Wilson[77] for both cases:

$$\sigma^2_{FT}(I_j) = I_j/t \qquad \text{for fixed time}$$
$$\sigma^2_{FC}(I_j) = I_j^2/C \qquad \text{for fixed counts} \tag{3.25}$$

The differential in Eq. 3.23 is now derived. Rewriting Eq. 3.17:

$$2\theta_p = 2\theta_o - \frac{\delta^2(n_2^2-n_o n_4)}{2n_2}\left\{M_1/(n_2\delta^2 M_o - n_o M_2)\right\} . \tag{3.26}$$

Now:

$$\frac{\partial 2\theta_p}{\partial I_j} = \frac{\partial 2\theta_p}{\partial M_i}\cdot\frac{\partial M_i}{\partial I_j} \quad \text{where} \quad \frac{\partial M_i}{\partial I_j} = \delta^{i+1}j^i \tag{3.27}$$

$$\frac{\partial 2\theta_p}{\partial I_j} = \frac{-\delta^2(n_2^2-n_o n_4)}{2n_2}\left\{\frac{(n_2\delta^2 M_o - n_o M_2)\delta^2 j - M_1(n_2\delta^3 j^0 - n_o\delta^3 j^2)}{(n_2\delta^2 M_o - n_o M_2)^2}\right\} \tag{3.28}$$

$$= \frac{-\delta^2(n_2^2-n_o n_4)}{2n_2(n_2\delta^2 M_o - n_o M_2)^2}\left\{n_o\delta^3 M_1 j^2 + (n_2\delta^2 M_o - n_o M_2)\delta^2 j - n_2\delta^3 M_1\right\} \tag{3.29}$$

Combining Eq. 3.23, 3.25 and 3.29 will give the error in peak location due to counting statistics alone.

For accumulation of data by fixed time (at each observation point j) the formula is:

$$\sigma^2(2\theta_p) = \frac{\delta^4(n_2^2-n_o n_4)^2}{4n_2^2(n_2\delta^2 M_o - n_o M_2)^4} \sum_{j=-n}^{n} (n_o\delta^3 M_1 j^2 + (n_2\delta^2 M_o - n_o M_2)\delta^2 j - n_2\delta^3 M_1)^2 I_j / t \qquad (3.30)$$

where $\sigma(2\theta_p)$ represents the standard deviation in the peak position. The assumption of a parabolic profile implies symmetry about the peak position. The term M_i represents an i^{th} moment of intensity about the peak. Wilson[63] suggests that because the profile has been considered symmetric (at least in the region fit by a parabola) the odd moments of intensity will be of less importance (for a perfect paracola the odd moments are zero) reducing Eq. 3.30 to:

$$\sigma^2(2\theta_p) = \frac{\delta^4(n_2^2-n_o n_4)^2}{4\cdot t\cdot n_2^2(n_2\delta^2 M_o - n_o M_2)^4} \sum_{j=-n}^{n} (n_2\delta^2 M_o - n_o M_2)^2 \delta^4 j^2 I_j$$

$$= \frac{\delta^4(n_2^2-n_o n_4)^2}{4\cdot t\cdot n_2^2(n_2\delta^2 M_o - n_o M_2)^2} \cdot \delta^4 \sum_{j=-n}^{n} j^2 I_j$$

$$= \frac{\delta^8(n_2^2-n_o n_4)^2 \cdot M_2}{4\cdot t\cdot n_2^2(n_2\delta^2 M_o - n_o M_2)^2} \qquad (3.31)$$

In the same manner, for data accumulated by fixed counts at each j:

$$\sigma^2(2\theta_p) = \frac{\delta^4(n_2^2-n_o n_4)^2}{4n_2^2(n_2\delta^2 M_o - n_o M_2)^4} \sum_{j=-n}^{n} (n_o\delta^3 M_1 j^2 + (n_2\delta^2 M_o - n_o M_2)\delta^2 j - n_2\delta^3 M_1^2) I_j^2 / C \qquad (3.23)$$

Neglecting the odd moments of intensity, Eq. 3.32 reduces to:

$$\sigma^2(2\theta_p) = \frac{\delta^8(n_2^2 - n_o n_4)^2}{4Cn_2(n_2\delta^2 M_o - n_o M_2)^2} \sum_{j=-n}^{n} j^2 I_j^2 \qquad (3.33)$$

3.4.3 Experimental Confirmation of the Statistical Formulae for Peak Location

The counting statistical errors for the peak location were examined with the 211 peak using three samples to cover a range of breadths; the 1090-1, 1045-1, and TBA G-5 specimens.

Three observation points were chosen from a chart scan of the profile and were within the top 15 pct of the peak intensity. Data was repeatedly accumulated using fixed counts at these same observation points 15 times for each sample and the peak position and statistical error (using Eq. 3.32) were calculated employing a computerized system.* The results are given in Table 3.5. The peak position is the average value of the 15 measurements. The standard deviation from the mean peak location, $S(2\theta_p)$ is given in column 3. When compared with the average counting statistical error (one standard deviation) given in column 4, it is seen that the correspondence is remarkable thereby showing that Eq. 3.32 for fixed count analysis predicts the proper counting error. The slight difference is probably due to missetting of 2θ because the limit of gearing accuracy on the Picker diffractometer is .002°2θ.

---

*The program as described in Chapter 4 was modified slightly to use the same angular position for the data points during the replicate tests. As will be seen in Chapter 4, the program normally selects these positions and in each measurement the different positions would affect these tests.

TABLE 3.5

ERROR ANALYSIS FOR REPEATED PEAK DETERMINATIONS $Cr_{K\alpha}$ - 211 PEAK
(15 Measurements)

Sample	$\langle 2\theta_p \rangle$ °2θ	$S(2\theta_p)$ °2θ	$\sigma(2\theta_p)$ °2θ
1090-1	156.184	.0022	.0021
1045-1	155.916	.0023	.0021
TBA G-5	155.282	.0112	.010

*$\langle 2\theta_p \rangle$ represents the mean value of the peak position.

$S(2\theta_p)$ represents the observed standard deviation from the mean value.

$\sigma(2\theta_p)$ is the counting statistical error.

3.4.4 Experimental Confirmation of the Approximate Formulae for the Variance in Peak Location

By assuming the actual data to be symmetric about the working origin, i.e., the center of the curve fitting region, Eq. 3.31 (for fixed time) and Eq. 3.33 (for fixed counts) were derived. A test of these approximations were made by analyzing data obtained from the $Cr_{K\alpha}$ 211 diffraction peak on steel samples. The tests were carried out for both $\psi=0^\circ$ and $\psi=45^\circ$ (after tilting the peak may be more asymmetric) using stationary slit geometry. The 1090-1 and TBA G-5 samples were used, the first exhibiting excellent $K_{\alpha 1}$-$K_{\alpha 2}$ separation with the second having no separation. Table 3.6 reproduces the results for the fixed count method. The number of data points is given in column 3 and the step increment between points, δ, is given in column 4. The breadth at half the maximum intensity is given in column 5.

Three data points from a peak of any shape can form a perfect parabola. Therefore, one would not expect any difference in the results between the exact formula and the approximation (based on perfect symmetry of the actual data) using three data points. This is seen to be so in Table 3.6 for both samples. With a multi-point fit, any asymmetry will be more evident. From Table 3.6, the difference between the results calculated by both formulae is negligible for the multipoint fit implying that the actual profile is symmetric about the peak location after the data has been corrected for the 2θ-dependent intensity factors. The exact formula is used in the computer program, STRESS described in Chapter 4.

3.5 STATISTICAL VARIANCE IN STRESS

The variance in the measured peak position results in an error in

TABLE 3.6

COMPARISON OF EXACT STATISTICAL FORMULAE TO APPROXIMATE FORMULAE FOR THE COUNTING ERROR IN PEAK LOCATION USING A PARABOLIC FIT*
(The data is corrected for Lorentz-Polarization and absorption factors as discussed in Sec. 3.2)

Sample	ψ Degrees	Number of Data Points	δ* °2θ	W °2θ	$\sigma(2\theta_p)$ Eq.3.32 (°2θ)	$\sigma(2\theta_p)$ Eq.3.33 (°2θ)	% Change in $\sigma(2\theta_p)$
1090-1	0	3	.11	.45	.00085	.00085	0
	0	7	.03	.45	.00105	.00105	0
	45	3	.15	.50	.00139	.00139	0
	45	7	.05	.50	.00181	.00180	.3
TBA G-5	0	3	2.83	6	.01023	.01023	0
	0	15	.38	6	.0134	.0133	.8
	45	3	2.35	6	.0147	.0147	0
	45	15	.38	6	.0146	.0144	1.37

*δ represents the 2θ step increment between data points. W is the full width at half the maximum intensity. The % change represent the pct difference in $2\theta_p$ between the statistical error as calculated from Eq. 3.2 and Eq. 3.3.

the calculated residual stress. This error will be derived for both the '$\sin^2\psi$' method and the 'two tilt' method.

3.5.1 '$\sin^2\psi$' Technique

In the '$\sin^2\psi$' technique the residual stress, σ_φ, is determined from the slope of the interplanar spacing $d_{\varphi,\psi}$ versus $\sin^2\psi$. The variance in $d_{\varphi,\psi}$ due to random errors in the measured intensities will introduce an error in the surface stress. The variance in $d_{\varphi,\psi}$ must be determined from the variance in $2\theta_p$.

Writing Bragg's law:

$$d = \lambda/2\sin\theta \tag{3.34}$$

Applying Eq. 3.20 to the relation in Eq. 3.34:

$$\sigma^2(d) = \left[\frac{\partial(\lambda/2\sin\theta)}{\partial\theta}\right]^2 \sigma^2(\theta)$$

$$= \left(\frac{\lambda\cos\theta}{2\sin^2\theta}\right)^2 \frac{\sigma^2(2\theta)}{2} \cdot \left(\frac{\pi}{180}\right)^2 \tag{3.35}$$

where 2θ is in degrees and $\sigma^2(2\theta)$ is given by any one of Eqs. 3.30 - 3.33.

The surface stress is given by m', the regression coefficient of $d_{\varphi,\psi}$ vs. $\sin^2\psi$. The regression coefficient of a linear least squares line is given by:[75]

$$m' = \frac{\Sigma(x_i-\bar{x})(y_i-\bar{y})}{\Sigma(x_i-\bar{x})^2} \tag{3.36}$$

where x_i is the independent variable and y_i is the dependent variable. The bar denotes averages. In terms of $d_{\varphi,\psi}$ and $\sin^2\psi$, the regression coefficient is expressed as:

$$m' = \frac{\sum_{\psi}(\sin^2\psi - \overline{\sin^2\psi})(d_{\varphi,\psi} - \overline{d_{\varphi,\psi}})}{\sum_{\psi}(\sin^2\psi - \overline{\sin^2\psi})^2} \tag{3.37}$$

where $$\overline{\sin^2\psi} = \sum_{\psi} \sin^2\psi / N$$

$$\overline{d_{\varphi,\psi}} = \sum_{\psi} d_{\varphi,\psi} / N$$

and N is the total number of observations.

The value of ψ also has finite error due to alignment and mechanical motion. The function $\sin^2\psi$ varies slowly so small errors in ψ have negligible effect on $\sin^2\psi$. The expression for the regression coefficient, Eq. 3.37 is then a linear function with the dependent variable having a predictable error. By application of Eq. 3.20, the variance of m' is:

$$\sigma^2(m') = \frac{\sum_{\psi}(\sin^2\psi - \overline{\sin^2\psi})^2 \cdot \sigma^2(d_{\varphi,\psi})}{\left[\sum_{\psi}(\sin^2\psi - \overline{\sin^2\psi})^2\right]^2} \tag{3.38}$$

where $\sigma^2(d_{\varphi,\psi})$ is given by Eq. 3.35. Through relation 3.20, the variance in the stress, σ_φ, (given by Eq. 1.5), is:

$$\sigma^2(\sigma_\varphi) = \sigma^2(m') / \left[d_o \cdot \frac{1+\nu}{E}\right]^2 \tag{3.39}$$

where $\sigma^2(m')$ is given by Eq. 3.38.

3.5.2 'Two Tilt' Technique

Application of Eq. 3.19 to the 'two tilt' method (given by Eq. 1.6) yields:

$$\sigma^2(\sigma_\varphi) = \left[\frac{\partial\sigma_\varphi}{\partial d_\psi}\right]^2 \sigma^2(d_\psi) + \left[\frac{\partial\sigma_\varphi}{\partial d_o}\right]^2 \sigma^2(d_o)$$

$$= \left[\frac{E}{1+\nu} \cdot \frac{1}{\sin^2\psi}\right]^2 \left(\frac{1}{d_o^2}\,\sigma^2(d_\psi) + \left(\frac{d_\psi}{d_o^2}\right)^2 \sigma^2(d_o)\right)$$

$$\approx \left(\frac{K}{d_o}\right)^2 \left[\sigma^2(d_\psi)+\sigma^2(d_o)\right] \qquad (3.40)$$

where the stress constant K is given by:

$$K = \frac{E}{1+\nu} \cdot \frac{1}{\sin^2\psi} \qquad (3.41)$$

If the peak shift is small, the two tilt equation can be expressed directly in terms of 2θ by Eq. 1.7. The variance in the surface residual stress is given by:

$$\sigma^2(\sigma_\varphi) = K'^2[\sigma^2(2\theta_o)+\sigma^2(2\theta_\psi)] \qquad (3.42)$$

where the variance in peak position is given by Eq. 3.30 or Eq. 3.32. Small errors in 2θ do not introduce significant error in the stress constant K', given by Eq. 1.8.

3.5.3 Comparison of Statistical Formulae for 'Two Tilt' Method

Kelly and Short[78] derived an equation for the error in the residual stress as determined using the 'two tilt' method due to

counting statistics. Using Eq. 1.8 and writing the peak location directly in terms of the counts at each of three data points (therefore using a three point fit) Kelly and Short obtained an equation relating the stress, σ_ϕ, directly to the intensity obtained at the three observation points. They applied Eq. 3.22 to this formulae to calculate the counting error. Defining (1-P) as the relative difference in intensity between the peak position and the outer observation points, and N as the total counts at each point, they obtained, for fixed count data accumulation:

$$\sigma(\sigma_\phi) \simeq K \cdot \Delta 2\theta \cdot \sqrt{P} / (2(1-P)\sqrt{N}) \qquad (3.43)$$

where K is the stress constant in Eq. 1.8. This equation is valid only for a three point parabola and the 'two tilt' method of residual stress analysis. Their derivation assumes the angular increment between data points to be identical for both ψ inclinations and also the same total counts are achieved at both ψ tilts.

Table 3.6 compares results obtained from analyzing the expected counting error with Eq. 3.42 and Eq. 3.43 from data taken on three steel specimens. The data was taken in the top 15% region using fixed counts. The samples were chosen to cover a range of peak breadths and residual stress levels.

The counting errors calculated by each equation are given in Table 3.7 and are similar, although exact agreement is not expected because of the assumptions made by Kelly and Short. The results do indicate the statistical error from both methods are comparable, however, the

TABLE 3.7

COMPARISON OF THE STATISTICAL ERROR IN RESIDUAL STRESS AS CALCULATED IN THIS STUDY AND BY KELLY AND SHORT[78]
Cr_{K_α} radiation - 211 peak - three point parabolic fit

Sample	σ_ϕ MPa	δ^* ° 2θ	1-P	$\sigma(\sigma_\phi)$, MPa Eq. 3.43	$\sigma(\sigma_\phi)$, MPa Eq. 3.42
1090-1	+12.8 (+1860 psi)	.11	.155	±1.97(140 psi)	±.875 (127 psi)
1045-1	-176 (-25,600 psi)	.295	.159	±3.49 (506 psi)	±3.14 (456 psi)
1045-2	-400 (-57,950 psi)	2.11	.172	±8.17 (1185 psi)	±8.96 (1300 psi)

* δ is the step increment between the angular positions of the data points.

lack of generality of the Kelly and Short analysis limits its application. Their derivation is based on the two tilt method for the residual stress determination and assumes the peak shift ($^{\circ}2\theta$) and stress are proportional. This is valid only for a small peak shift. The statistical analysis as developed in Sec. 3.4.2 enables the statistical error to be calculated for either the exact or approximate 'two tilt' formulae (Eq. 3.40 and Eq. 3.42, respectively) and for the '$\sin^2\psi$' method (Eq. 3.39).

3.5.4 Automated Residual Stress Program

A complete computer controlled residual stress analysis program was developed during this study. An in depth discussion of the program is given in Chapter 4, but because the program is used in the remaining sections of Chapter 3 the program is described briefly here to facilitate the reader's understanding.

The residual stress program incorporates the following features which are chosen by the user by means of an initial dialog:

1) The experimental parameters are input (approximate peak location, divergent slit, sample displacement and ψ-axis missetting) to calculate geometric aberrations.

2) Either the 'two tilt' or '$\sin^2\psi$' methods of residual stress analysis may be applied, with a normal detector or the PSD.

3) The Marion-Cohen technique is implemented automatically if a least-squares fit to d vs. $\sin^2\psi$ indicates oscillations.

4) The operator specifies the desired accuracy in terms of degrees 2θ for each peak or in stress and the counting strategy is determined taking into account both statistical and geometric errors.

5) The peak is fit to a parabola by a least-squares procedure. The operator specifies the number of data points to be fit.

6) If desired, background is measured and subtracted.

7) Either parafocusing or stationary-slit geometry can be chosen.

8) An estimate of the overall time of analysis is given after a preliminary scan of the peak. The operator can then change the error if the time is too long.

Five successive step scans are involved in the procedure for determining a peak position, as described below. The data is collected in fixed count mode and corrected for deadtime and angular dependent intensity factors.

1) A step scan is made in large increments ($\sim .2°2\theta$) set by the operator, accumulating 1000 counts at each position from the initial 2θ, until a count rate of less than 90 pct of the maximum is obtained.

2) Two step scans follow in smaller increments (set initially by the user and typically 0.05°) down each side of the peak to locate two angles, $2\theta_1$ and $2\theta_3$ at 85 pct of the maximum intensity. (The background measured at an angular position specified by the user, may be subtracted from the data in determining the two end points. This procedure serves to define the region of parabolic fit more accurately.)

3) A third step scan at the two angles from Step 2 and the central angle between them is made with a preset count of 5000. A three point parabola is fit to the data. Then angles are calculated for the desired number of data points such that the central data point will be very close to the center of the parabolic fit. This minimizes odd order terms in the error equations. These preliminary scans typically take 60 seconds.

4) A step-scan at the final angular positions for a preset 1000 counts is used to back calculate the necessary counts from Equation 3.32 to obtain the desired precision. Steps 3 and 4 constitute a multiple pass procedure which serves to improve the reliability of peak location and minimize the time required for a given precision.

5) The final data is acquired for the calculated preset counts at each angular position.

3.6 EXPERIMENTAL DETERMINATION OF THE PRECISION OF RESIDUAL STRESS ANALYSIS

3.6.1 Introduction

A complete statistical analysis of the peak location using a least-squares parabolic fit to the top of a diffraction profile has been presented. While useful in determining random errors due to counting statistics, other factors also contribute to the precision of the measurement. The experimental technique (i.e., 'two tilt' vs. '$\sin^2\psi$' methods) and accuracy of the equipment influence the overall precision.

The actual precision has been examined in this study under varying conditions. The reproducibility of residual stress determination using a least squares parabolic curve for peak location is compared to that using a three point parabola. The precision of the 'two tilt' method and '$\sin^2\psi$' method are examined and compared to each other. These treatments on precision have apparently never before been carried out.

The reproducibility of residual stress determination using a position sensitive detector (PSD) for data accumulation is also examined. The precision is dependent on the resolution and stability of the PSD and these are shown to be quite adequate for residual stress analysis by X-ray diffraction.

The precision of the residual stress measurement is dependent of the method of peak location. Traditionally in X-ray stress measurements using a diffractometer, the apex of a three point parabola fit to the top region of the diffraction profile is used to define the Bragg angle as has been mentioned several times. It was shown in Sec. 3.4.3 that the region near the maximum of the profile is symmetric about the peak position after Lorentz-polarization and absorption factors are made, verifying the practicality of the three point parabola compared to a least-squares approach. Jatczak and Boehm[29] conclude that a more elaborate fitting of 2nd, 3rd and 4th order curves to five data points produces good agreement with the three point parabola method and hence was not worth the extra time needed in accumulating the data. However, Marion[30] found a least-squares parabolic fit to 10 to 20 data points gave better reproducibility than just the three point fit. This apparent contradiction is important to resolve because the curve fitting procedure will affect the precision. It is obvious that many data points are preferable to only a few given unlimited time. For a fixed total time, however, this is not necessarily true. Yap[67] concluded that if the profile is a perfect parabola the optimum procedure for collecting data is to spend most of the time at the two end points of the parabola and only a short time at the peak in a three-point fit. Since random errors dictate that the observed data is not a perfect parabola the effect of the number of observation points on the precision was experimentally tested in this study. The total time for data accumulation was fixed and tests were run using the 'two tilt' method in the following manner:

1) Fix the total time spent accumulating the data.

2) Determine the time at each point. Counting can be accomplished in either fixed time or fixed count mode.

3) Repeat the measurement until enough results have been accumulated to check the reproducibility.

4) Duplicate steps 2 and 3 for a different number of data points, keeping the total time of measurement constant.

By varying the number of data points, the effect of this number on the precision can be assessed.

3.6.2 Experimental Procedure

An automated diffractometer system was used to accomplish the repeated measurements. The system is comprised of a Picker diffractometer and scintillation detector interfaced to a PDP-8E computer. A position sensitive detector was also used in conjunction with the diffractometer. The features of the software programming are described in Sec. 3.5.4. The only modification of the program for these tests concerned the procedure for determining the fixed counts accumulated at each observation point. In its usual form, the computer program allows the operator to chose the desired number of data points and determines the necessary counting time to achieve a designated statistical precision. Since the total time of data accumulation must be fixed for each peak determination in this analysis, the following procedure was substituted. Defining the total time as T, the fixed counts at each observation point, j, as CT, and the power in counts/second at each j as IN(j), the average power times total time will yield the total counts. Dividing this by the number of data points, N, yields an average fixed counts. Therefore:

$$CT = \frac{T \cdot \overline{IN(j)}}{N} \qquad (3.44)$$

where $\overline{IN(j)}$ represents an average intensity in CPS. The individual IN(j) are determined initially from a rapid step scan used to determine the position of the observation points through the use of the 'top 15 pct' rule. The total time, T, was input and the program determined CT.

For the position sensitive detector, the total time is fixed by the multichannel analyzer which acts as a peripheral storage device for the data so it was not necessary to alter the usual computer program.

The samples were chosen to cover a broad spectrum of residual stresses and breadths of diffraction profiles.

3.6.3 The Effect of the Number of Data Points

Ten repeated stress measurements were made on each of the steel samples for each number of observation points. Three, five, seven, eleven and fifteen observations in the region of curve fitting were used. The diffractometer alignment was checked and the sample positioned for minimum sample displacement prior to beginning the measurements on each sample. No instrumental changes were made during the replicate testing.

The 'two tilt' method using ψ angles of 0° and 45° was employed with a stress constant of 593 MPa/°2θ (86000 psi/°2θ).[7] The stationary slit or non-focusing technique was used so as not to include random errors due to repositioning of the receiving slit (see Sec. 3.2.2 for more details on the effect of slit positioning).

Table 3.8 summarizes the effect of the number of data points employed to determine the peak maximum on the precision with a normal detector and the two tilt procedure. The number of data points, column 2 and the total time of data accumulation for the two tilts,* column 3, were set in the initial dialog with the computer program. The residual stress given in column 4 is the average value over 10 measurements. The observed error, one standard deviation from the mean stress for the 10 replicate measurements is given in column 5 and the statistical counting error for one standard deviation (Eq. 3.42) is given in the last column.

The data for the 1090-1 sample which exhibits a sharp 211 diffraction profile with excellent $K_{\alpha 1}$-$K_{\alpha 2}$ separation illustrates that for such a profile, the number of data points has little effect on the precision. The counting error is slightly less than the observed precision, as expected. For this sample the precision is approximately ±1.4 MPa (±200 psi), better than that usually reported in the literature (± 10 MPa)[7] because the peak was very sharp.

As the breadth of the diffraction profile increases the peak position becomes more sensitive to small fluctuations in the data and the counting statistics for the three point fit do not predict the true error. But as the number of data points in the least-squares fit increase, the observed precision once again approaches the counting error. These results show that counting statistics are not a good measure of the precision when using only three points for a parabolic fit on samples having broad profiles. Only where the number of data points is increased is the observed precision represented by this

*The total time is for the final step scan only and does not include the time spent in the preliminary scans as this is independent of the number of data points.

TABLE 3.8

RESULTS OF FIXED TIME TESTS
(TWO TILT METHOD)

	Number of Data Points	Total Time (sec)	Stress MPa (psi)	Observed Error 10 Tests MPa (psi)	Statistical Error 10 Tests Eq. 3.42 MPa (psi)
1090-1 (W=.45)*	3	360	32.3 (+4690)	±1.40 (±203)	±0.97 (±141)
	5	360	31.6 (+4580)	± .82 (±119)	±1.18 (±171)
	7	360	31.0 (+4500)	±1.21 (±173)	±1.22 (±177)
	11	360	31.4 (+4550)	±1.54 (±223)	±1.34 (±195)
1045-1 (W=1.50)	3	360	-179.8 (-26080)	±10.04 (±1457)	±3.45 (±500)
	5	360	-176.6 (-25620)	±10.98 (±1574)	±3.96 (±574)
	7	360	-167.3 (-24266)	± 6.89 (±1000)	±4.02 (±583)
	11	360	-165.4 (-23997)	± 6.38 (± 926)	±4.31 (±625)
	15	360	-165.2 (-23967)	± 6.12 (± 888)	±4.33 (±628)
1045-3 (W=3.40)	3	1000	-699.5 (-101470)	±13.70 (±1987)	±4.57 (±663)
	5	1000	-700.3 (-101508)	±11.44 (±1660)	±6.20 (±899)
	7	1000	-700.1 (-101556)	± 9.29 (±1347)	±6.71 (±973)
	11	1000	-697.0 (-101100)	± 6.28 (± 911)	±7.35 (±1066)
	15	1000	-699.3 (-101432)	± 6.57 (± 953)	±7.43 (±1077)
1045-2 (W=5.1)	3	1000	-395.7 (-57396)	±28.68 (±4160)	±9.34 (±1325)
	5	1000	-400.4 (-58082	±14.41 (±2090)	±11.79 (±1710)
	7	1000	-399.6 (-57958)	±13.27 (±1925)	±13.06 (±1894)
	11	1000	-395.9 (-57408)	±11.20 (±1624)	±13.51 (±1959)
	15	1000	-394.0 (-57107	±12.80 (±1857)	±14.13 (±2049)
TBA G-5 (W=5.8)	3	1000	+15.9 (+2300)	±33.77 (±4898)	±9.21 (±1336)
	5	1000	+15.2 (+2200)	±21.37 (±3099)	±11.27 (±1635)
	7	1000	+13.1 (+1898)	±15.69 (±2276)	±11.90 (±1726)
	11	1000	+11.2 (+1621)	±12.80 (±1856)	±12.40 (±1799)
	15	1000	+12.6 (+1829)	±12.34 (±1791)	±12.53 (±1818)
1090-2 (W=6.0)	3	1000	-354.2 (-51375)	±38.00 (±5513)	±12.20 (±1770)
	5	1000	-351.9 (-50140)	±36.97 (±5362)	±14.82 (±2150)
	7	1000	-343.0 (-49760)	±23.10 (±3351)	±15.68 (±2275)
	11	1000	-342.4 (-49660)	±17.56 (±2547)	±16.41 (±2380)
	15	1000	-345.1 (-50060)	±17.48 (±2536)	±16.30 (±2365)

*W represents the breadth at half the maximum intensity in °2θ.

counting error. This phenomena becomes especially pronounced for broad profiles; e.g., compare the 1045-2, TBA G-5 and 1090-2 samples in Table 3.7.

The reason for this result becomes apparent when one examines the entire procedure for locating the peak position. Say the positions of the observation points were found only once and for each repeated measurement the data was taken for the specified time at these same observation points. One would expect the observed error for the three point fit to be identical with the counting error for the 10 measurements. Indeed, this was shown to be the case in Sec. 3.4.3.

If, however, during each measurement the position of the data points are rechosen, as is the case here because of the automation employed for collecting the data in Table 3.8, the position of the data points change due to random fluctuations in the observed intensities. Only if the actual data were a <u>perfect</u> parabola would one expect the observed and counting errors to be identical. This might lead one to think the profile must not be a perfect parabola in the region used for the curve fit. It was seen in Sec. 3.3.3 that not subtracting the background can lead to errors in the determination of the region of fit of the parabola. As the breadth increases, the ratio of peak intensity to background intensity decreases for these samples (see Table 2.2) causing the region of fit as determined by the 'top 15 pct' rule to be too large. The data does not, then, necessarily lie on a parabola.

When a least-squares multiple point fit is used, the relative effect of those points lying outside the true region of the parabola

is decreased causing the observed error to decrease, although the same total time of data accumulation is used. Surprisingly the statistical counting error increases probably because the degree of perfection of the parabolic fit decreases with increasing number of data points. This is due to random fluctuations in the data which dictate that the observed data cannot exactly lie on a parabolic curve.

To determine if the region of curve fitting actually effects the reproducibility, replicate measurements were made on the 1045-1, 1045-2 and TBA G-5 samples using the same total time as in Table 3.8 but including a background correction (see Sec. 4.3.4 for details on automated background subtraction) prior to determining the region of fit. The two tilt method using a three point parabolic curve to define the peak location was used. The results given in Table 3.9 indicate an improvement by a factor of almost two in the observed error as compared to Table 3.8 for the samples exhibiting broad profiles when using a three point parabolic fit. However, the precision for the 1045-2 and TBA G-5 samples was still almost twice that predicted by counting statistics alone, again indicating that the three point fit is not adequate for fitting broad profiles.

3.6.4 Comparison of '$\sin^2\psi$' Method to 'Two Tilt' Method

The $\sin^2\psi$ method involves measurement of the peak position at more than two inclinations which could minimzie the random errors associated with individual measurements of the peak. For a fixed total time, the time spent at each ψ tilt will be less than in the two-tilt method, thereby increasing the statistical error of the peak location so

TABLE 3.9

RESULTS OF REPLICATE FIXED TIME TESTS USING BACKGROUND SUBTRACTION
(two-tilt, three point parabolic fit to peak)

Sample	Total Time (sec)	Stress MPa (psi)	Observed Error 10 Test MPa (psi)	Statistical Error Eq. 3.42 MPa (psi)
1045-1	360	-169.0 (-24520)	± 4.58 (± 605)	±3.86 (± 560)
1045-2	1000	-408.5 (-59260)	±14.44 (±2095)	±9.41 (±1365)
TBA G-5	1000	+11.17 (+1620)	±17.48 (±2535)	±9.79 (±1420)

that one cannot say a priori whether or not the $\sin^2\psi$ method is more precise.*

The precision of the $\sin^2\psi$ method was determined in the same manner as described for the two tilt method, the total time of data accumulation being identical. Only a three point parabolic fit (no background subtraction) was employed, the ten replicate measurements being made on the 1045-1, 1045-2 and TBA G-5 samples with ψ tilts of 0°, 26.57°, 39.23° and 50.77°.

If the results given in Table 3.10 are compared to those in Table 3.8, it is seen that the $\sin^2\psi$ technique has better precision (observed error) over the ten measurements than the two tilt technique even when the <u>total</u> time of data accumulation is identical. The effect of errors in peak location are minimized with multiple tilts. Increasing the number of ψ inclinations to more than four was tested but improvement in the precision was only nominal. The standard error in the mean stress (column 4, Table 3.10) is still 30 pct greater than that predicted by counting statistics (column 5) for the three point fit on the broader profiled samples.

The best results when using a three point parabolic fit could be expected to be found by combining both the '$\sin^2\psi$' method and using a background correction in determining the region of peak fit. Ten replicate measurements were taken in this manner on the same samples and using the same fixed time as in Table 3.10. The results from such measurements are given in Table 3.11. The precision is indeed improved and compares quite well with that expected from counting statistics alone.

---

*This entire discussion assumes that the d_ψ vs. $\sin^2\psi$ data falls on a straight line so that the two tilt method is valid and accurate. If d_ψ vs. $\sin^2\psi$ were not linear, the Marion-Cohen method would have to be used to account for the oscillations due to deformation texturing.

TABLE 3.10

PRECISION USING $\sin^2\psi$ METHOD
(three point parabolic fit to peak)

Sample	Total Time (sec)	Stress MPa (psi)	Observed Error 10 Tests MPa (psi)	Statistical Error Eq. 3.39 MPa (psi)
1045-1	360	-193.0 (-27990)	± 5.65 (± 820)	± 5.97 (± 866)
1045-2	1000	-402.8 (-58430)	±15.93 (±2310)	±10.90 (±1581)
TBA G-5	1000	+ 22.8 (+ 3300)	±18.13 (±2630)	±14.48 (±2100)

TABLE 3.11

PRECISION USING $\sin^2\psi$ METHOD AND BACKGROUND CORRECTION
(three point parabolic fit to peak)

Sample	Total Time (sec)	Stress MPa (psi)	Observed Error 10 Tests MPa (psi)	Statistical Error Eq. 3.39 MPa (psi)
1045-1	360	-199.60 (-28952)	± 6.19 (± 898)	± 4.78 (± 694)
1045-2	1000	-424.20 (-61529)	±11.17 (±1620)	±10.61 (±1539)
TBA G-5	1000	+ 14.71 (+ 2134)	±16.13 (±2340)	±16.65 (±2415)

3.6.5 Precision Obtained Using a Position Sensitive Detector

In Sec. 3.6.3 it was shown that many data points within the region of curve fitting improved the observed precision of the stress measurement for a parabolic curve. The position sensitive detector (PSD) collects data simultaneously across the diffraction profile and therefore does not take any longer period of time in collecting many points compared to just three. The number of data points collected in a fixed period of time depends solely on the breadth of the diffraction peak and a least-squares parabolic fit may be made to all those points falling within the appropriate region.

Replicate measurements were made with the PSD to test the actual precision. The automated residual stress program was used without any modifications. The fixed time of analysis was pre-determined by the time selected on the multichannel analyzer (MCA) which acted as an intermediate storage device for the data from the PSD. The MCA was interfaced with the PDP-8E computer for direct data transfer.

The computer program determined the region of curve fitting by the 'top 15 pct' of the intensity profile without subtracting background and fit a least-squares parabola to all data within the region. Column 2, Table 3.12 gives the number of data points within the region of curve fitting. The two tilt method was utilized, the total time of both tilts being recorded in column 3 of Table 3.12.

The results tabulated in Table 3.12 indicate that the accuracy of the PSD system is excellent. The observed error (column 5) in the mean stress is very close to that predicted by the counting statistics (column 6) alone. Thus the $\sin^2\psi$ method is not needed if the 'two tilt'

TABLE 3.12

PRECISION OBTAINED WITH A POSITION SENSITIVE DETECTOR
(Two-Tilt Method)

Sample	Number of Data Points	Time (sec)	Stress MPa (psi)	Observed Error 10 Tests MPa (psi)	Statistical Error MPa (psi)
1090-1	15	100	23.89 (+ 3465)	6.34 (± 920)	4.48 (± 650)
1045-1	31	100	198.6 (-28800)	5.72 (± 830)	4.34 (± 630)
1045-3	87	200	718.4 (-104200)	7.38 (±1070)	6.87 (± 995)
1045-2	141	200	412.3 (-59800)	9.20 (±1335)	9.69 (±1405)
TBA G-5	196	200	22.75 (+ 3300)	13.03 (±1890)	13.86 (±2010)

method is accurate (see Sec. 1.2). Obtaining many data points (column 2) within the region of parabolic fit eliminates the necessity for subtracting background. The best precision obtained with the normal detector comes from using the $\sin^2\psi$ method and subtracting background. The time for the final data collection for this procedure (not including the 60 seconds or so taken during the preliminary scans) is given in Table 3.11 and can be compared with the total time of analysis using the PSD in Table 3.12. This demonstrates the remarkable speed of the PSD, even when only a normal X-ray tube is used.

3.7 STUDIES OF SAMPLE DISPLACEMENT

Perhaps the largest single source of instrumental error associated with the X-ray measurement of residual stresses is sample displacement. In focusing geometry, if the effective diffracting volume is not located at the center of the diffraction circle, there is a relative shift between $\psi=0^\circ$ and $\psi=\psi^\circ$ given by Eq. 3.6. The error due to a given displacement is dependent on R_p', the position of the receiving slit. The equation is valid for both the parafocusing and stationary-slit techniques and is experimentally tested below. The parallel beam technique discussed in Sec. 3.2.2 does not employ a receiving slit to define the angular relationship between the primary and diffracted beam. The angular relationship depends solely on the angle between the parallel Soller slits mounted 90° to the diffractometer plane and does not depend on the position of the sample, thereby eliminating the error caused by sample displacement.

The effect of sample displacement was tested for each of the "beam optics" techniques. The positioning of the sample was accurate

to within ± .0025 mm. Three replicate measurements were made at each sample position up to a total displacement of ± 2 mm* in increments of .5 mm using the automated residual stress program. The 1045-1 sample was utilized because it gave a reasonably sharp profile. The residual stress was measured using the two tilt procedure and a three point parabolic fit without background correction.

The parallel beam method was obtained by placing two sets of high reslution Picker Soller slits together in both the incident and diffracted beams and rotated 90° to the usual position. This yielded a divergence of .5° similar to the values used in Japan.[27] Such slit systems were placed in the primary and diffracted beams.

The error for both the parafocusing and stationary slit methods predicted by Eq. 3.6 are drawn as solid lines in Fig. 3.7. The experimental data given in Fig. 3.7 for each technique closely follows the predicted error. The stationary slit technique is seen to be less susceptible to sample displacement by almost a factor of five over the parafocusing technique.

The parallel beam geometry is seen to be insensitive to reasonable sample displacements in agreement with Aoyama, et al.[68] [Of course, if the sample is displaced far enough, the diffracted beam will not fall completely in the receiving Soller slits introducing a large error.] The parallel beam technique decreases the intensities by about ½ and broadens the diffraction profile. This instrumental broadening is most important on samples exhibiting sharp profiles when focusing geometry is used. The reproducibility or precision of the parallel beam technique was tested.

---

*A negative displacement is defined as being towards the back surface of the sample.

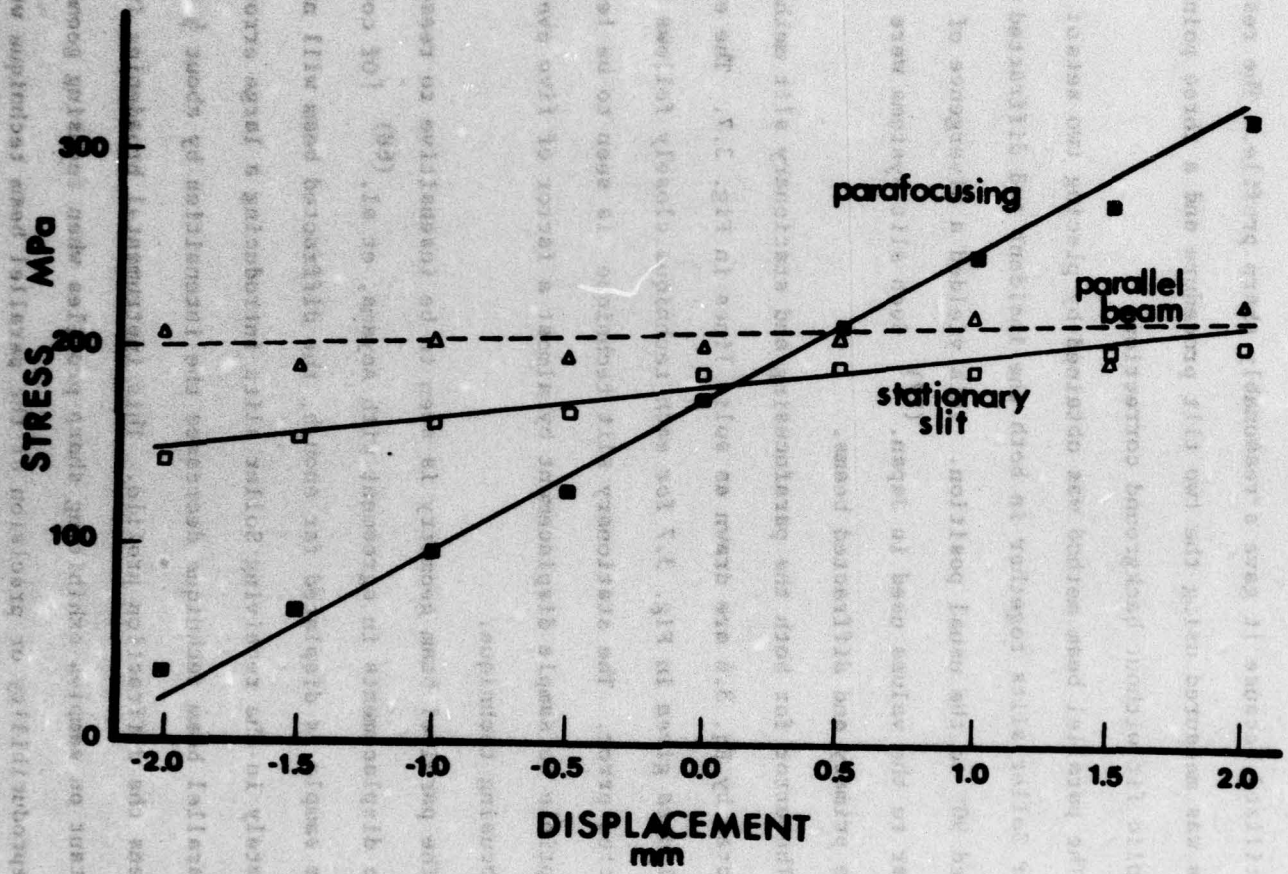

FIGURE 3.7 The dependence of stress on sample displacement for three geometric focusing techniques, 1045-1 sample. The solid lines represent the error as calculated from Eq. 3.6. The dashed line represents the slope of the actual data with a parallel beam.

The data for Table 3.13 was acquired for a fixed time to give a statistical error close to that in Table 3.8 using the two tilt procedure and a three point fit (no subtraction of background). The precision for the 1045-1 is twice as poor but approaches that of the focusing techniques for samples having broad profiles. The time of analysis is 1/3 longer for approximately the same statistical error for all specimens.

3.8 SUMMARY

A review of the important biasing factors in the residual stress measurement by X-ray diffraction techniques has been presented. The effect of sample displacement has been treated experimentally verifying the formulae used to predict this error. It was seen that stationary slit 'beam optics' is less susceptible to sample displacement than parafocusing geometry and has less instrumental broadening than the parallel beam method. This indicates the stationary slit method is the best 'beam optics' arrangement when applied to X-ray residual stress measurements.

A complete statistical analysis for the error in stress due to counting statistics was presented. The analysis was made as general as possible and includes unlimited data points in the peak region and use of either two tilt or '$\sin^2\psi$' procedures.

It has been shown experimentally that the three point parabola (which is traditionally used because of its simplicity) is justified only when the region of curve fit is determined accurately. If the background level is high compared with the peak intensity, it must be subtracted prior to determining the region of fit using the 'top 15 pct' rule. Even if this is accomplished, a three point fit is not very precise when broad profiles are involved. By using multiple data points

TABLE 3.13

PRECISION USING PARALLEL BEAM GEOMETRY
(Two Tilt Procedure - Three Point Parabolic Fit to Peak)
(10 Measurements)

Sample	Breadth (°2θ)	Time (sec)	Stress MPa (psi)	Observed Error MPa (psi)	Statistical Error MPa (psi)
1045-1	2.1	500	-161.0 (- 23360)	±15.50 (±2245)	± 4.03 (± 585)
1045-3	3.8	1300	-702.6 (-101920)	±16.55 (±2400)	± 5.03 (± 730)
1045-2	5.3	1300	-417.3 (- 60525)	±39.68 (±4450)	± 7.07 (±1025)
TBA G-5	6.0	1300	+ 11.6 (+ 1682)	±24.92 (±3615)	±16.82 (±2440)

and a least-squares parabola on broad profiles the reproducibility of peak location can be improved by a factor of three without increasing the total time of data accumulation. The practical necessity of using a computer to perform the least-squares analysis detracts from using multiple data points, however, when complete automation is available this type of analysis is worthwhile. In addition, the practical advantage of multiple data points increases the appeal of a position sensitive detector where such data is accumulated simultaneously.

Surprisingly, when only a three point fit is used, the $\sin^2\psi$ method is shown to be more reproducible than the two tilt method even if the total time is fixed in both procedures. Clearly, if true automation is to be achieved with optimum procedures, a least-squares parabola to define the peak or the $\sin^2\psi$ method of analysis must be used.

REFERENCES

1. Nondestructive Evaluation of Residual Stress, Proceedings of a Workshop, Air Force Materials Laboratory, NTIAC-76-2, Southwest Research Center, San Antonio, Texas (1976).

2. E. W. Weinman, J. E. Hunter, and D. D. McCormack, Metal Progress, 96 No. 1, 88 (1969).

3. K. Kamachi , X-Ray Study on Strength and Deformation of Metals, The Society of Materials Science, Japan (1971), p. 95.

4. C. S. Barrett and T. B. Massalski, Structure of Metals, 3rd Edition, McGraw Hill, New York (1966), p. 466-485.

5. B. D. Cullity, Elements of X-Ray Diffraction, Addison-Wesley Publ. Co., Reading, MA. (1956), p. 431-451.

6. H. P. Klug and L. E. Alexander, X-Ray Diffraction Procedures, John Wiley and Sons, Inc., New York (1974) p. 755-790.

7. Residual Stress Measurement by X-Ray Diffraction-SAE J 784a, 2nd Edition, Society of Automotive Engineers, Inc. (1971).

8. G. B. Greenough, Prog. in Metal Physics, 3, 176 (1952).

9. S. Taira, K. Hayashi and Z. Watase, Proceedings of the Twelfth Japan Congress on Materials Research, The Society of Materials Science, Japan, 1 (1970).

10. T. Shiraiwa and Y. Sakamoto, Proceedings of the Thirteenth Japan Congress on Materials Research, The Society of Materials Science, Japan, 25 (1971).

11. E. Macherauch, Proc. 3rd. Int. Conf. Nondes. Test., 720 (1961) Tokyo, Japan.

12. A. Ruess, Z. Angew, Math. Mech., 9, p. 48-58 (1929).

13. W. Voight, Lehrbuch der Kristallphysik, Teubner, Leipzig/Berlin, (1928).

14. E. Kroner, Z. Phys., 151, p. 504-508, (1958).

15. F. Bollenrath, V. Hauk, and E. H. Müller, Z. Metallkunde, 58, p. 76-82 (1967).

16. N. Hosokawa, K. Honda, and J. Arima, Mechanical Behavior of Materials, (Proceedings of the Inter. Conference), The Society of Materials Science, Japan, p. 164-175 (1972), Kyoto, Japan.

17. J. T. Norton, Adv. in X-Ray Analysis, 11, p. 401 (1967).

18. R. E. Ricklefs and W. P. Evans, Adv. in X-Ray Analysis, 10, p. 273 (1966).

19. R. H. Marion and J. B. Cohen, Adv. in X-Ray Analysis, 18, p. 466 (1974).

20. T. Shiraiwa and Y. Sakamoto, X-Ray Study on Strength and Deformation of Metals, The Society of Materials Science, Japan, (1971) p. 15.

21. F. Bollenrath, V. Hauk, and W. Ohly, Z. Metallkunde, 57, p. 464 (1966).

22. M. J. Donachie and J. T. Norton, Trans AIME, 221, p. 962 (1961).

23. F. Bollenrath, V. Hauk and W. Weidemann, Archiv für das Eisenhütt, 38 793 (1967).

24. W. Weidemann, Ph.D. thesis, Technische Hochschule, Aachen, Germany (1966).

25. K. W. Andrews, J. C. Gregory and D. Brooksbank, Strain, 10, 111 (1974).

26. D. P. Koistinen and R. E. Marburger, Trans ASM, 51, 537 (1959).

27. X-Ray Studies on Mechanical Behavior of Metals, The Society of Materials Science, Japan, Kyoto, Japan (1974) p. 72.

28. M. Short and C. Kelly, Adv. in X-Ray Analysis, 16, 379 (1972).

29. C. Jatczak and H. Boehm, Adv. in X-Ray Analysis, 17, 354 (1973).

30. R. H. Marion, Ph.D. thesis, Northwestern University, 1973.

31. C. Jatczak and H. Zantopulos, Adv. in X-Ray Analysis, 14, 360 (1970).

32. Residual Stress Measurements by X-Ray Diffraction - SAE J784a, 2nd Edition, Society of Automotive Engineers, Inc. (1971) p. 71.

33. J. B. Cohen, Diffraction Methods in Materials Science, MacMillan Co., New York (1966) p. 294.

34. K. H. Lauterjung, J. Pokar, B. Schimmer, and R. Staudner, Nucl. Inst. and Meth., 22, 117 (1963).

35. R. Bock, H. H. Duhn, W. Melzer, F. Dulilhofer, and B. Stadler, Nucl. Inst. and Meth., 41, 190 (1966).

36. S. Kalbitzer and W. Melzer, Nucl. Inst. and Meth., 56, 30 (1967).

37. W. W. Daehnick, Phys. Rev., 177, 1795 (1967).

38. D. L. Alan, G. V. Arsell, and R. K. Kelly, Atomic Energy Research Est., Harwell, Berkshire Report AERE-R5897 (1968).

39. A. Doehring, S. Kalbitzer, and W. Melzer, Nucl. Inst. and Meth. 59, 40 (1968).

40. R. B. Owen and M. L. Awcock, IEEE Trans. Nucl. Sci., NS-15, 290 (1968).

41. U. Beble and F. Parah, Nucl. Inst. and Meth., 112, 455 (1973).

42. W. R. Kuhlmann, K. H. Lauterjung, B. Schimmer, and L. Sistermich, Nucl. Inst. and Meth., 40, 118 (1966).

43. W. N. McDichen, Nucl. Inst. and Meth., 54, 157 (1967).

44. C. J. Borkowski and M. K. Kopp, Rev. Sci. Inst., 39, 1515 (1968).

45. C. J. Borkowski and M. K. Kopp, IEEE Trans. Nucl. Sci., 17, 340 (1970).

46. J. Hough and A. Drever, Nucl. Inst. and Meth., 103, 365 (1973).

47. H. Foeth, R. Hammerstrom, and C. Rubbia, Nucl, Inst. and Meth., 109, 521 (1973).

48. D. G. Smith and K. A. Pounds, IEEE Trans. Nucl. Sci., 15, 541 (1968).

49. R. Gott, W. Parks and K. A. Pounds, Nucl. Inst. and Meth., 81, 152 (1970).

50. J. Hough, Nucl. Inst. and Meth., 105, 323 (1972).

51. G. I. Miller, A. Senator, and R. Stensgraad, Nucl. Inst. and Meth., 91, 389 (1971).

52. G. P. Westphal, Nucl. Inst. and Meth., 106, 279 (1973).

53. H. W. Fulbright, R. G. Markham, and W. A. Langford, Nucl. Inst. and Meth., 108, 125 (1973).

54. J. L. C. Ford, J. Gomes, Del Campo, R. L. Robinson, B. H. Stelson, and S. T. Thornton, Nuclear Physics, A226, 189 (1974).

55. A. Gabriel and S. Bram, Febs. Letters, 39, 307 (1974).

56. Y. Dupont, A. Gabriel, MChabre, T. Gulik-Krzywicki, and E. Schechter, Nature, 238, 331 (1972).

57. E. Mathieson, Nucl. Inst. and Meth., 97, 171 (1971).

58. H. P. Klug and L. E. Alexander, X-Ray Diffraction Procedures, John Wiley and Sons, Inc., New York (1974) p. 329.

59. Ibid., p. 635.

60. F. Y. Yap, dissertation (The John Hopkins University, Baltimore, Maryland, 1967).

61. A. J. C. Wilson, Acta. Cryst. 23, 888 (1967).

62. J. Thomsen and F. Y. Yap, J. of Research of Nat. Bureau of Standards, 72A, 187 (1968).

63. A. J. C. Wilson, Brit. J. Apply. Phys., 16, 665 (1965).

64. M. J. Cooper and A. V. Glasspool, J. Apply. Cryst. 9, 63 (1976).

65. International Tables for X-Ray Crystallography, Vol. III, Kynoch Press, Birmingham, England (1968).

66. J. B. Cohen, "Report on Tungsten Lattice Parameter Round Robin," X-Ray Subcommittee of SAE Iron and Steel Technical Committee, Division 4, (November 1964).

67. J. Fukura and H. Fujiwara, J. of the Society of Materials Science, Japan, 15, 825 (1966).

68. S. Aoyama, K. Satta and M. Tada, J. of the Society of Materials Science, Japan, 17, 1071 (1968).

69. D. N. French, J. Amer. Cer. Soc., 52, 271 (1969).

70. W. E. Baucum and A. M. Ammons, Adv. in X-Ray Analysis, 17, 371 (1973).

71. "Standard Method for X-Ray Stress Measurement", The Committee on Mechanical Behavior of Materials, The Society of Materials Science, Japan (1973).

72. Residual Stress Measurements by X-Ray Diffraction-SAE J784a, 2nd Edition, Society of Automotive Engineers, Inc., (1971), p. 51.

73. J. Sekita, K. Oguro, U. Kaminago and Y. Oguro, X-Ray Study on Strength and Deformation of Metals, The Society of Materials Science, Japan (1971) p. 81.

74. A. J. C. Wilson, Mathematical Theory of X-Ray Powder Diffractometry, Philips Technical Library (1963).

75. W. Parrish and T. C. Huang, Profile Tilting: A Powerful Method of Computor X-Ray Instrumentation and Analysis, IBM Research (1976).

76. O. Davies and P. Goldsmith, Statistical Methods in Research and Production, Hafner Publ. Co., New York (1952) p. 72.

77. X-Ray Diffraction, Ed. L. Azaroff, McGraw Hill, New York (1974) p. 439.

Security Classification

DOCUMENT CONTROL DATA - R & D

(Security classification of title, body of abstract and indexing annotation must be entered when the overall report is classified)

1. ORIGINATING ACTIVITY (Corporate author)	2a. REPORT SECURITY CLASSIFICATION
J. B. Cohen, Northwestern University, Evanston, IL	Unclassified
	2b. GROUP

3. REPORT TITLE

EVALUATION OF PROCEDURES IN AUTOMATED RESIDUAL STRESS MEASUREMENTS

4. DESCRIPTIVE NOTES (Type of report and inclusive dates)

Technical Report No. 14

5. AUTHOR(S) (First name, middle initial, last name)

M. R. James and J. B. Cohen

6. REPORT DATE	7a. TOTAL NO. OF PAGES	7b. NO. OF REFS
N00014-75-C-0580 NR 031-733	80	77

8a. CONTRACT OR GRANT NO.	9a. ORIGINATOR'S REPORT NUMBER(S)
5345-455	Technical Report No. 14
b. PROJECT NO.	
c.	9b. OTHER REPORT NO(S) (Any other numbers that may be assigned this report)
d.	None

10. DISTRIBUTION STATEMENT

Distribution of this document is unlimited.

11. SUPPLEMENTARY NOTES	12. SPONSORING MILITARY ACTIVITY
	Office of Naval Research Metallurgy Branch

13. ABSTRACT

The measurement of residual stress by the X-ray diffraction technique involves determining the lattice spacing of a crystallographic plane at different inclinations of the sample and relating the change in the spacing to a stress on the surface of the specimen. The sources of error in determining the residual stress are investigated in this report. A short review of the fundamental principles of the measurement is given. The important instrumental and geometric factors contributing to errors in the measured stress are presented. To account for random errors in the data accumulation on the measured stress, a complete statistical analysis based on a least-squares parabola is given.

Employing an automated diffractometer (see T.R. No. 16), an extensive investigation of the precision of the residual stress measurement was made to evaluate the various procedures offered in the literature to optimize the automation. The results indicate that a multiple least-squares parabola is the most reproducible method of defining the peak of the profile, in contrast to the common three point parabola used in the United States, the center of gravity used in Germany or the middle of the half-maximum intensity used in Japan. Also, for a standard diffractometer, the $\sin^2\psi$ technique is more precise than the usual two tilt method even when the total time of analysis for each is identical. In studying various beam optic arrangements, it was found that the stationary slit (non-focusing method) offers the best system in that the measured stress is only mildly sensitive to sample displacement ($\sim$ 7 MPa for .25 mm displacement) and introduces very little instrumental broadening. The operational principles and use of a position sensitive detector (PSD) for the measurement of residual stress are included.

DD FORM 1 NOV 68 1473 (PAGE 1)

S/N 0101-807-6801

Unclassified

Security Classification

Unclassified

Security Classification

14. KEY WORDS	LINK A		LINK B		LINK C	
	ROLE	WT	ROLE	WT	ROLE	WT
stresses						
residual stresses						
automated stress measurements						
position sensitive detector						